BEHAVIOUR OF RIGID FOUNDATION ON HOMOGENEOUS LOOSE SOIL

Data report on tests BG-01 to BG-03

Barnali Ghosh & S.P.G. Madabhushi

CUED/D-SOILS/TR-330

TABLE OF CONTENTS

LIST OF FIGURES

LIST OF TABLES

1. Introduction

Routine design of raft foundations is based on the consideration of bearing capacity, settlement and uplift pressure. However, during earthquake induced liquefaction the seismic behaviour of the soil supporting the raft foundation will change the overall performance of the foundation. This often results in the tilting of the structure as a whole with the superstructure remaining intact as seen in Figure 1. Here the building which rested on a very rigid raft was toppled due to loss of support from the underlying soil during the Kocaeli earthquake. Yasuda & Berrill (2000) studied case histories of foundation failure after several earthquakes. In the field case histories the roles of individual parameters in causing observed failure is unknown, although the parameters influencing the overall behaviour of the structure maybe known. If a controlled model test is performed in the laboratory, the role of particular parameters in the observed failure pattern can be ascertained to a large extent. Thus, a series of controlled dynamic centrifuge tests was performed and the failure pattern observed in the field was replicated. This technical report investigates the behaviour of the soil – structure system under such incipient failure conditions.

Figure 1: Liquefaction induced bearing capacity failure in the Kocaeli earthquake (Photo courtesy NISEE website, University of California, Berkeley).

The present series of centrifuge tests are aimed at studying the SSI effects for a symmetric heavy base, low centre of gravity type structure founded on homogeneous liquefiable soil. The structure rests on a rigid raft where the interaction will be appreciable due to the maximum stiffness contrast between the raft and the foundation soil. The aim of these experiments is to characterize the soil response in terms of the measured accelerations and excess pore pressures which, lead to excessive settlement and failure. The test series involved 4 saturated tests and their general configuration is presented in Table 1.

Table 1: Test scheme

Test identification	Ground stratification	Embedment	Average relative density	Comments
BG-01	Uniform liquefiable soil	1.5m	54%	Consistency of the test compared with BG-02
BG-02	Uniform liquefiable soil	1.5m	55%	Pressure cells used to measure the soil pressure
BG-03	Uniform liquefiable soil	3m	54%	Increased the embedment.
BG-06(a) BG-06(b)	Uniform loose Medium loose	No structure 0.5m	56% 64%	Without structure With structure

2. Design of model structure & foundation

The design of the model containment was arrived at after considering the different combinations of materials that would give the desired bearing pressure and stiffness. The final dimensions of the containment were somewhat restricted by the size of the available ESB box. This was necessary to separate the free field behaviour (ideally 5 to 7 times the width of the base raft) from the behaviour under the structure.

Table 2: Structural Properties of model containment at model scale

Part	L (mm)	B (mm)	H (mm)	Volume (mm^3)	Density kg/ m^3	Mass (kg)
Raft	60	60	31.5	113400	7850	0.890
Hollow cylinder	Ext dia. 50.1	Int dia. 28.1	30	29100	2800	0.08156
Dome	Ext dia. 50.1	Int dia 28.1	25.4	27300	2800	0.0764
Mass of building at model scale: 1.085 kg, Bearing pressure at 1g 2.95kPa, Location of c.g 22 mm from base.						

Table 2 shows the structural properties of the different materials used in designing the model structure. The embedded raft foundation plate made from steel and the dome was made of dural (aluminium alloy). The total bearing pressure was 148 kPa at 50g. Figure 2 shows the model structure with its foundation. The superstructure is very rigid having a very low natural time period. The h/r ratio for the building is 1.65 where h is the height of the containment and r is the effective radius for an equivalent circular foundation. Such low value of h/r suggests that rocking during seismic shaking is unlikely and horizontal mode of vibration will dominate.

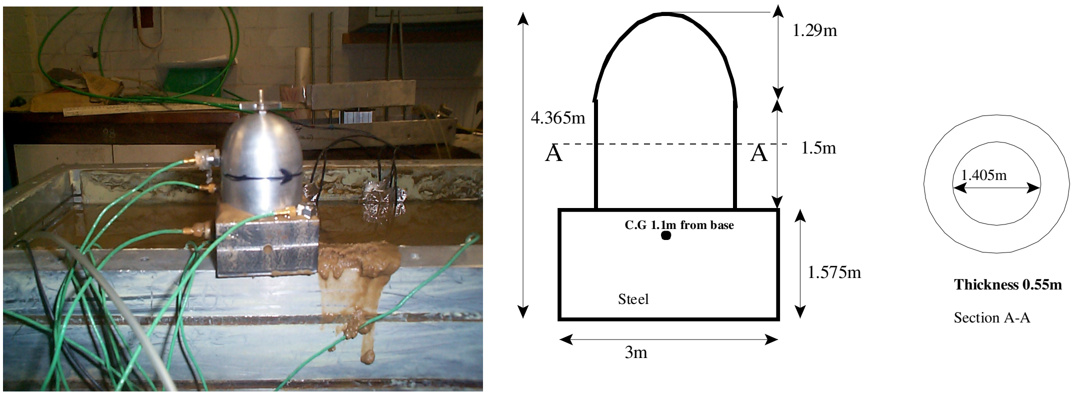

Figure 2: Model structure and its dimension in prototype scale.

3. Test layout & instrumentation (BG-01, BG-02, and BG-03)

Figure 3 and 4 presents the instrumentation layout at prototype scale for tests BG-01 and BG-02. The general instrument location was motivated by the fact that there should be a dense array of instrumentation close to the structure. The instrumentation in these tests consisted of accelerometers, pore pressure transducers and LVDT's. The initial models were essentially loose to medium relative density sand, which was expected to liquefy under medium and strong earthquakes. Table 3 presents the instrument locations in prototype scale.

In BG-02 attempts were made to measure the vertical pressure using earth pressure cells. As reported by several investigators (Clayton et al. 1993), it is extremely difficult to measure total stress in soil, so the results have to be viewed with caution. The pressure cells were arranged in such a way that they were coincident with the assumed load dispersion lines obtained from elastic solutions. Special care was taken of the earth pressure transducers that were buried in the liquefiable saturated sand.

One of the other interests in this tests series was to investigate the effects of embedment on the overall seismic response. The embedment depth was varied in the tests. In BG-03 the embedment was 3m and lateral pressures were measured during the shaking using earth pressure cells as shown in Figure 5 as the main horizontal interaction force is provided by direct stress on the walls of the foundation. These cells were glued to the edges of the base raft with double-sided tape to secure their positions. A series of earthquakes was fired at 50g for each model. Each shaking event was followed by a stationary period to allow for dissipation of the developed excess pore pressures.

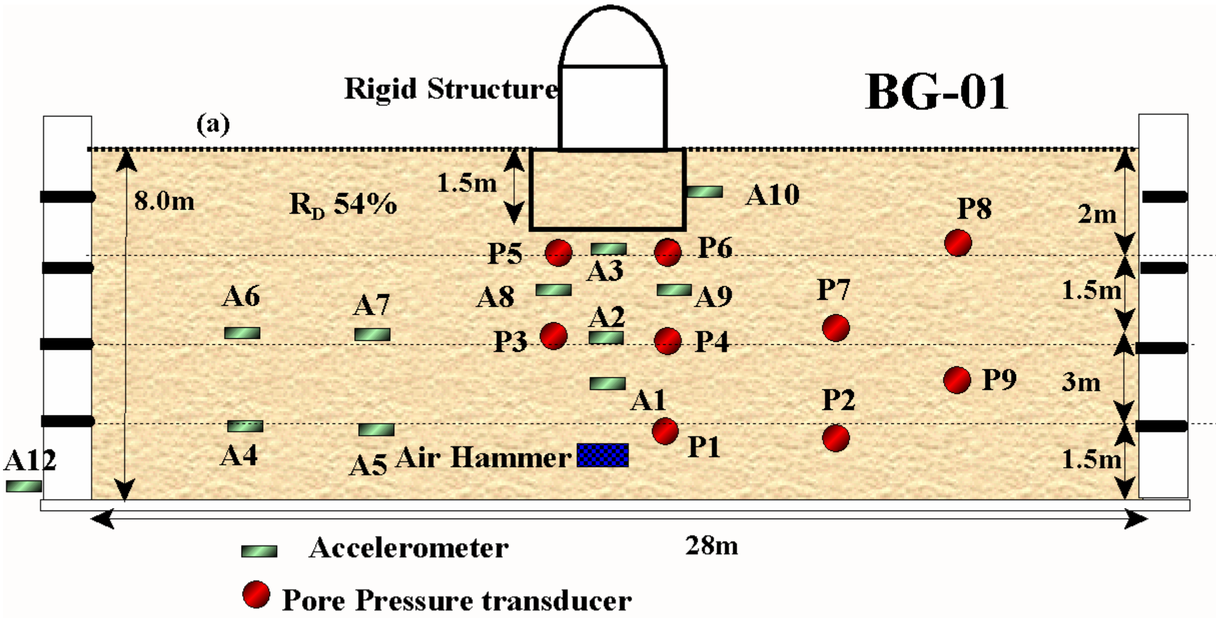

Figure 3: Instrumentation and test layout of BG-01.

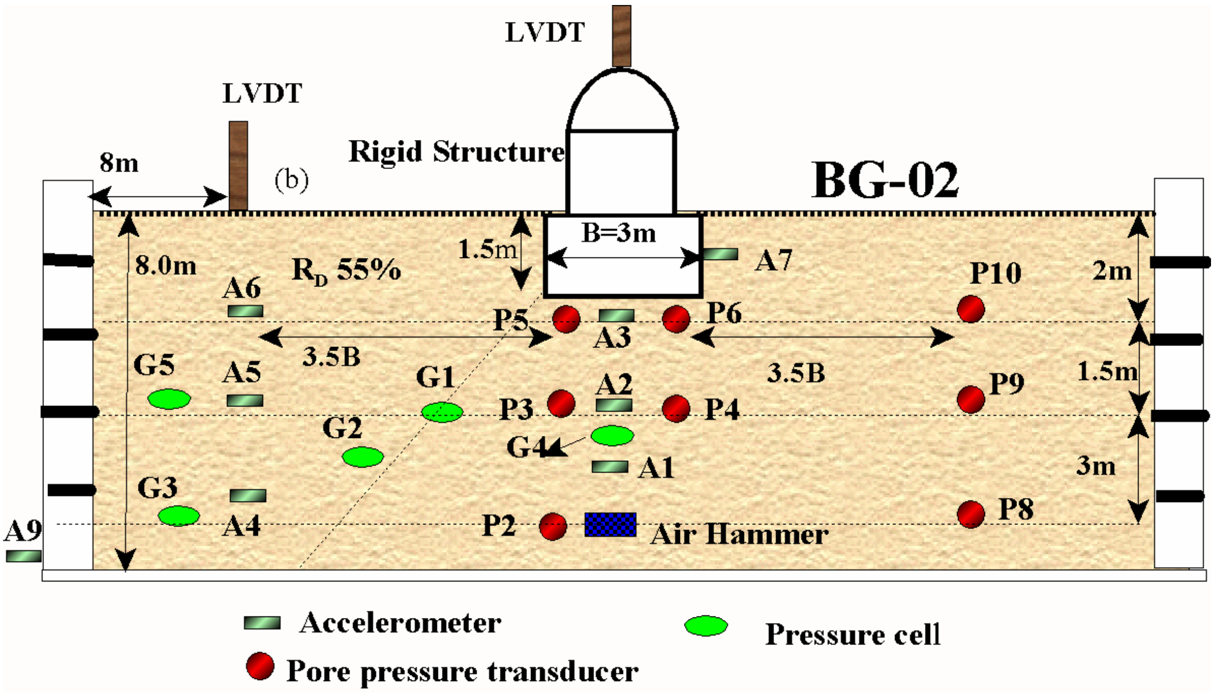

Figure 4: Instrumentation and test layout of BG-02.

Table 3: Instrument identification for test BG-01.

Instrument Identification	X (Along the length of ESB) (m)	Y (Along the width of the ESB) (m)	Z (Height from the top of the soil surface) (m)
A1	14	5.8	5
A2	13.75	5.8	3.45
A3	13.60	5.8	2
A4	5.75	5.6	6.85
A5	10.5	5.6	6.85
A6	5.8	5.64	3.5
A7	10.45	5.6	3.5
A8	13	5.5	3.25
A9	15.5	5.5	3.2
A10	On the structure		
A12	Input acceleration		
P1	16.5	5.7	6.75
P2	21.5	5.65	6.72
P3	13	5.7	3.5
P4	15.5	5.875	3.45
P5	13.2	5.875	2
P6	15.5	5.875	2
P7	21.25	5.8	3.5
P8	22	5.8	2
P9	22	5.75	4.75

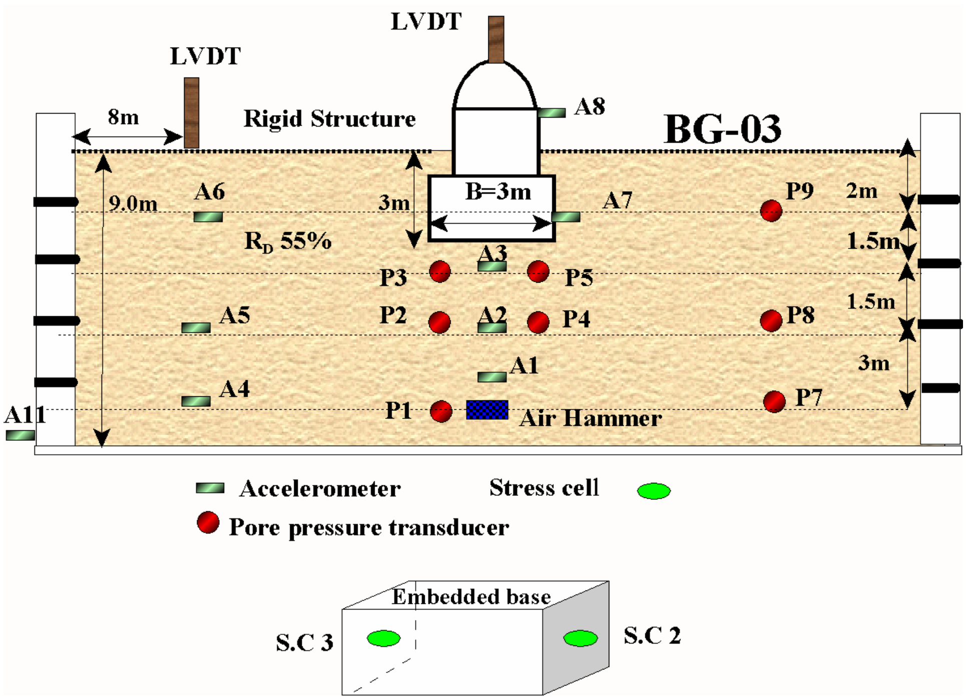

Figure 5: Instrumentation and test layout for test BG-03; Stress cell 4 and 5 are underneath the base of the raft foundation.

4. Visual observations after the tests

In sands, the very high stress levels required for bearing failure often shift the limiting design criterion to settlement. The settlement and tilting of the foundation are commonly considered as serviceability criteria. It was seen in the tests that following the sequence of earthquakes the structure had tilted and rotated as is seen after typical earthquake damage. Figure 6 shows the post-test observations for tests BG-02 and BG-03. For the sake of comparison tilt is defined as the rigid body rotation of the structure. In the experiments tilt is measured with respect to the rotation of the dome top in the clockwise or anticlockwise direction. After the tests, translation of the dome top in the direction of the tilt was carefully measured and used to calculate the approximate angle of rotation. The angle of rotation varied from 15 to 20°.

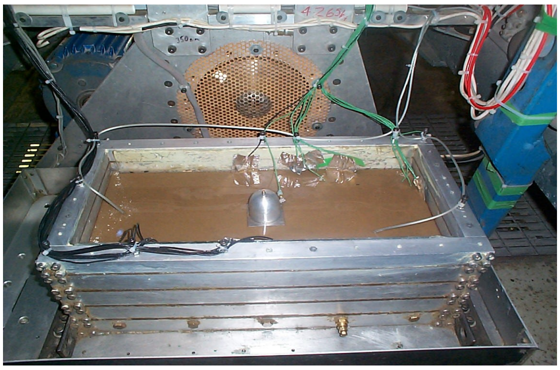

Initial position before earthquake (BG-02)

Tilt and rotation of dome after test BG-02

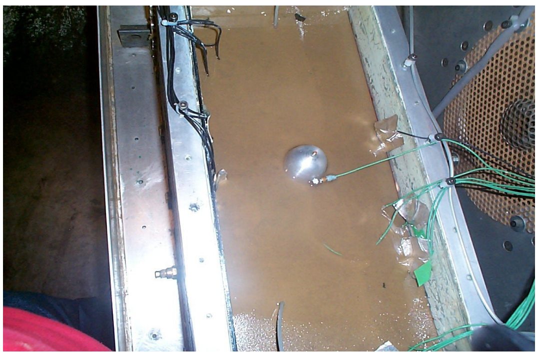

Tilt and rotation in BG-03

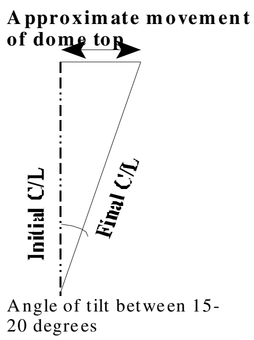

Figure 6: Post-test observation in tests BG-02 and BG-03.

5. Test Results

The test results are presented in Figure 7 to 34. In these tests DASYLab was used as a trial data acquisition system during the earthquake shaking to measure the response of the accelerometers (Ghosh 2003). Unfortunately the electromagnetic field of the SAM motor creates excessive interference and an unsatisfactory level of noise has been observed during trials. Thus the quality of data obtained from the accelerometer is very noisy despite using a 8^{th} order Butterworth filter. All the test results are presented in model scale.

5.1 Test BG-01

The results from this test are presented in Figure 7 to 10. The rigid foundation tilted after the earthquake shaking was imparted to the base of the model. The accelerations measured underneath the raft foundation were comparatively less attenuated in comparison to the free field attenuation. The excess pore pressure measured underneath the raft foundation did not reach the free field effective stress levels. The final tilt was about 20°.

5.2 Test BG-02

The test result from this series is presented in Figure 11 to Figure 21. The pore pressure recordings are different underneath the raft foundation. In the zone where the foundation tilted the excess pore pressures reveal the creation of a dilation zone which prevents complete toppling of the foundation. The acceleration data from this test is not very good as there was excessive interference from the SAM motor during the measurements.

5.3 Test BG-03

Figure 22 to 33 presents the accelerations and the pore pressure measurements recorded during test BG-03. In this test the embedment depth was varied and the test results show that greater embedment depth resulted in limiting the settlement of the structure. In addition to this the accelerations measured at the base of the structure was attenuated more in this case.

6. Conclusions

These three tests were the benchmark test to compare the results obtained from the tests on layered soil. In general it was seen that following the onset of liquefaction, the bedrock acceleration was attenuated as it travelled towards the surface. The isolation capabilities of the liquefiable layer was evident in all the test results.

7. Acknowledgements

I would like to acknowledge the help that I received from the technicians at the Schofield Centre in performing these tests. The advice from Dr. Stuart Haigh and Dr. Andrew Brennan is gratefully acknowledged.

8. References

Yasuda, S., Berrill, J.B., (2000), "*Observations of the earthquake response of foundations in soil profiles containing saturated sands*", Conference Proceedings of GeoEng 2000: An International Conference on Geotechnical and Geological Engineering, 19-24 November, Melbourne, Australia,1-30.

Clayton, C.R.I. & Bica, A.V.D.,(1993), "*The design of diaphragm type boundary total cells*", Géotechnique No.43(4),523-535.

Ghosh. B.(2003), " *Behaviour of rigid foundation in layered soil during seismic liquefaction*", PhD thesis, Cambridge University.

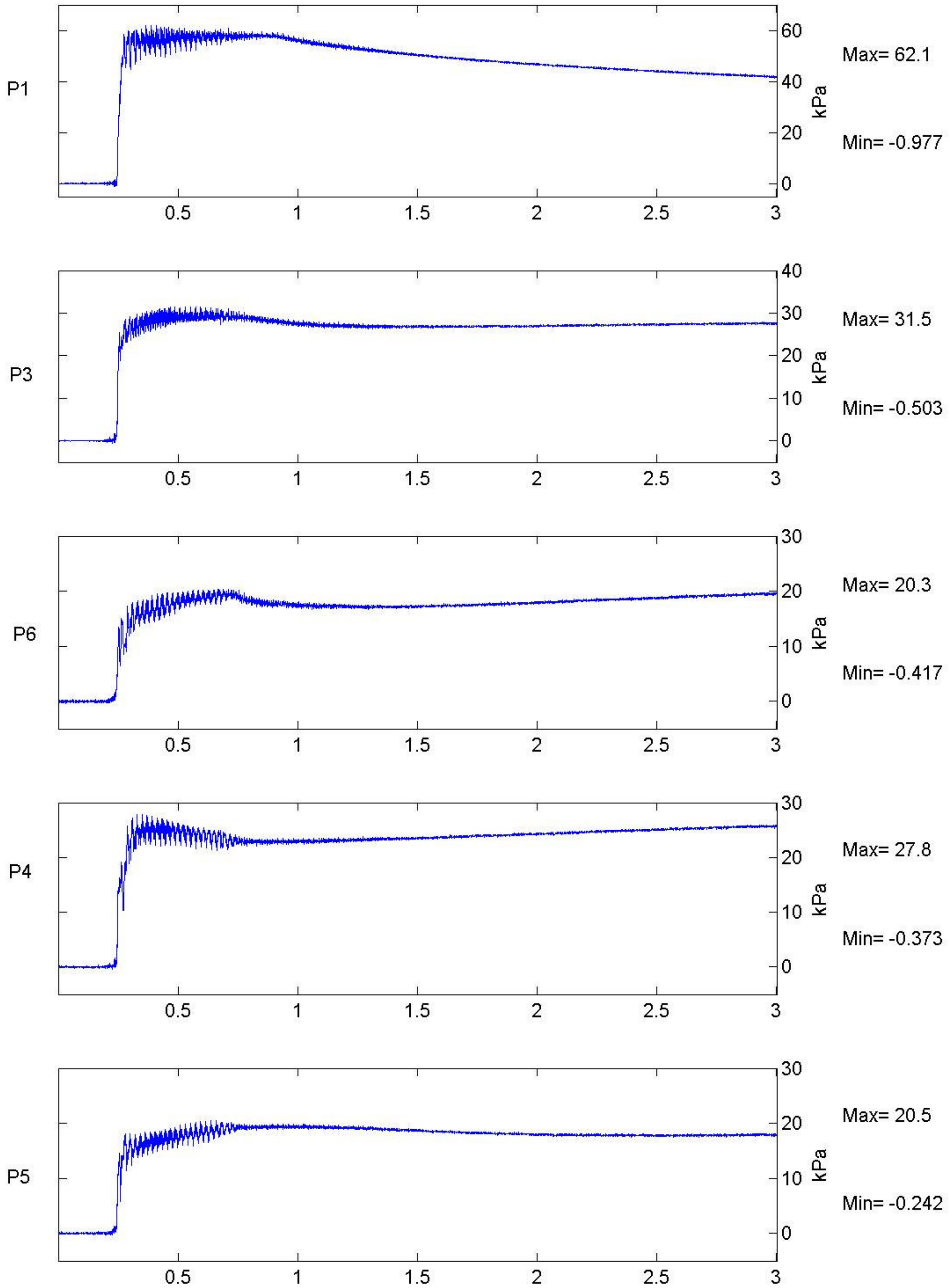

TEST BG-1 FLIGHT 1	**FREQ** **50 Hz**	Scales: Model Unfiltered Data Long-Term Time Records	Earthquake 1	Figure No. 7

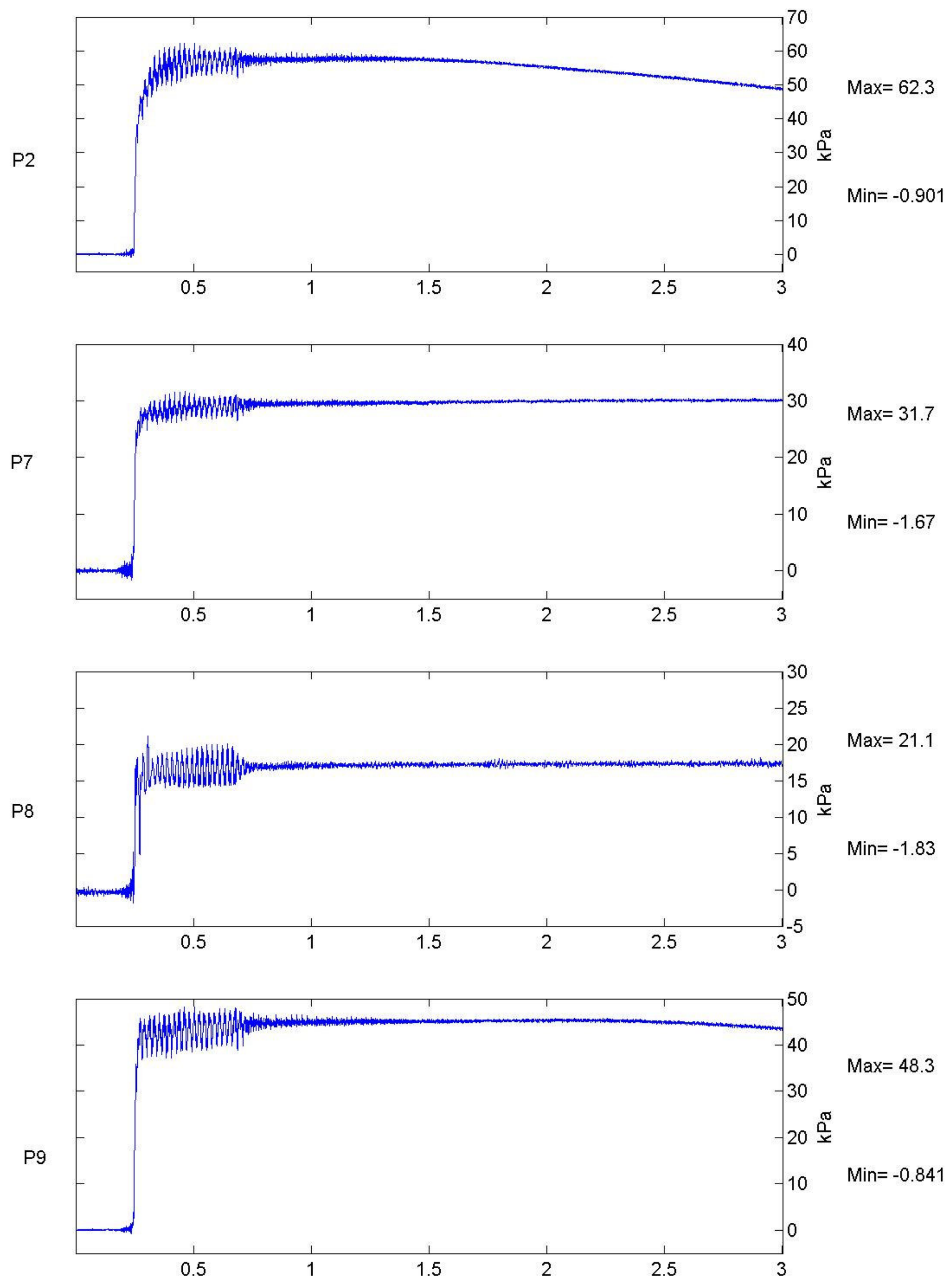

TEST BG-1	**FREQ**	Scales: Model	Earthquake	Figure No.
	50 Hz	Unfiltered Data		
FLIGHT 1		Long-Term Time Records	1	8

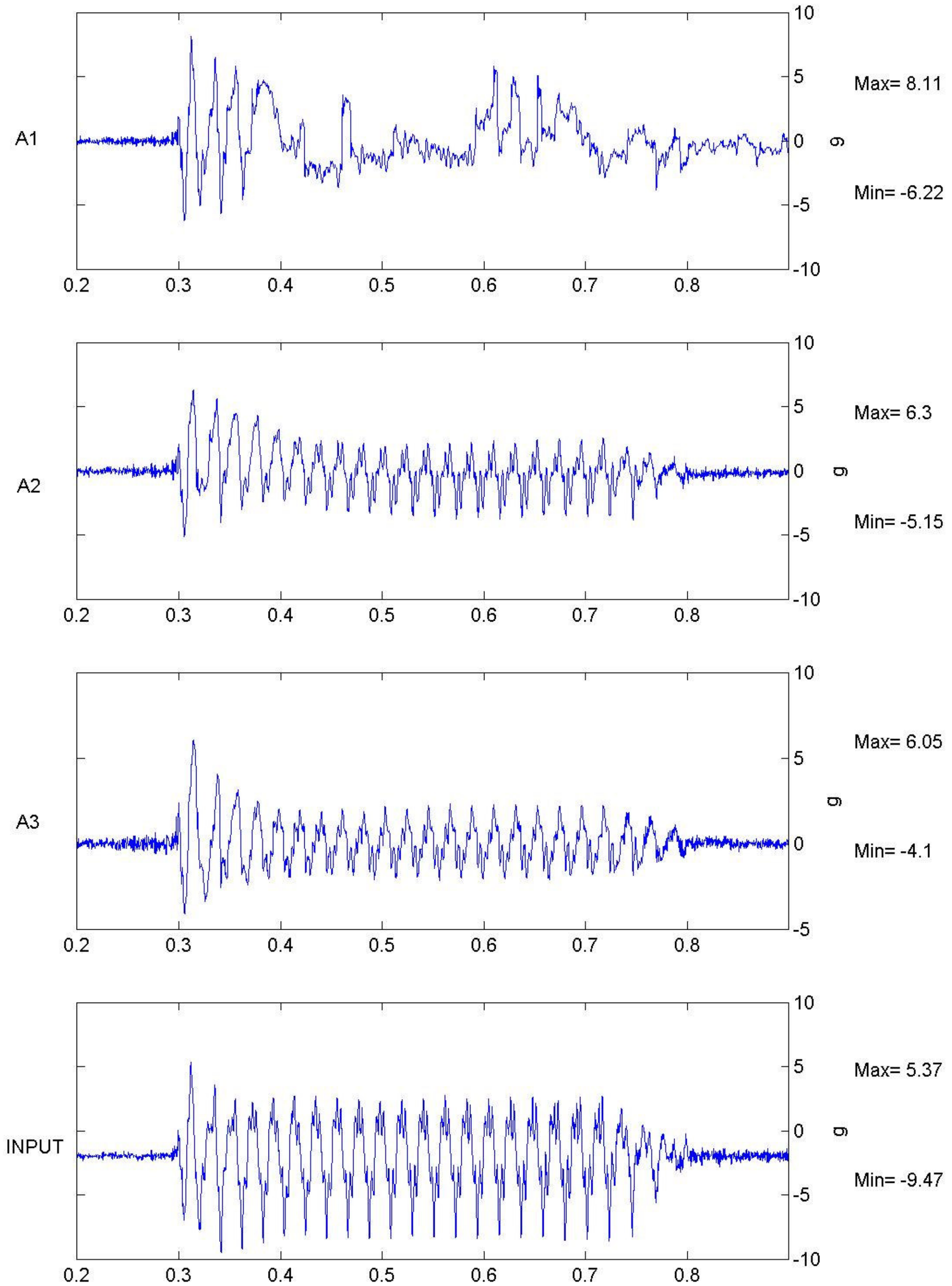

TEST BG-1 FLIGHT 1	**FREQ 50 Hz**	Scales: Model 8th order Butterworth Filter at 1000Hz Short-Term Time Records	Earthquake 1	Figure No. 9

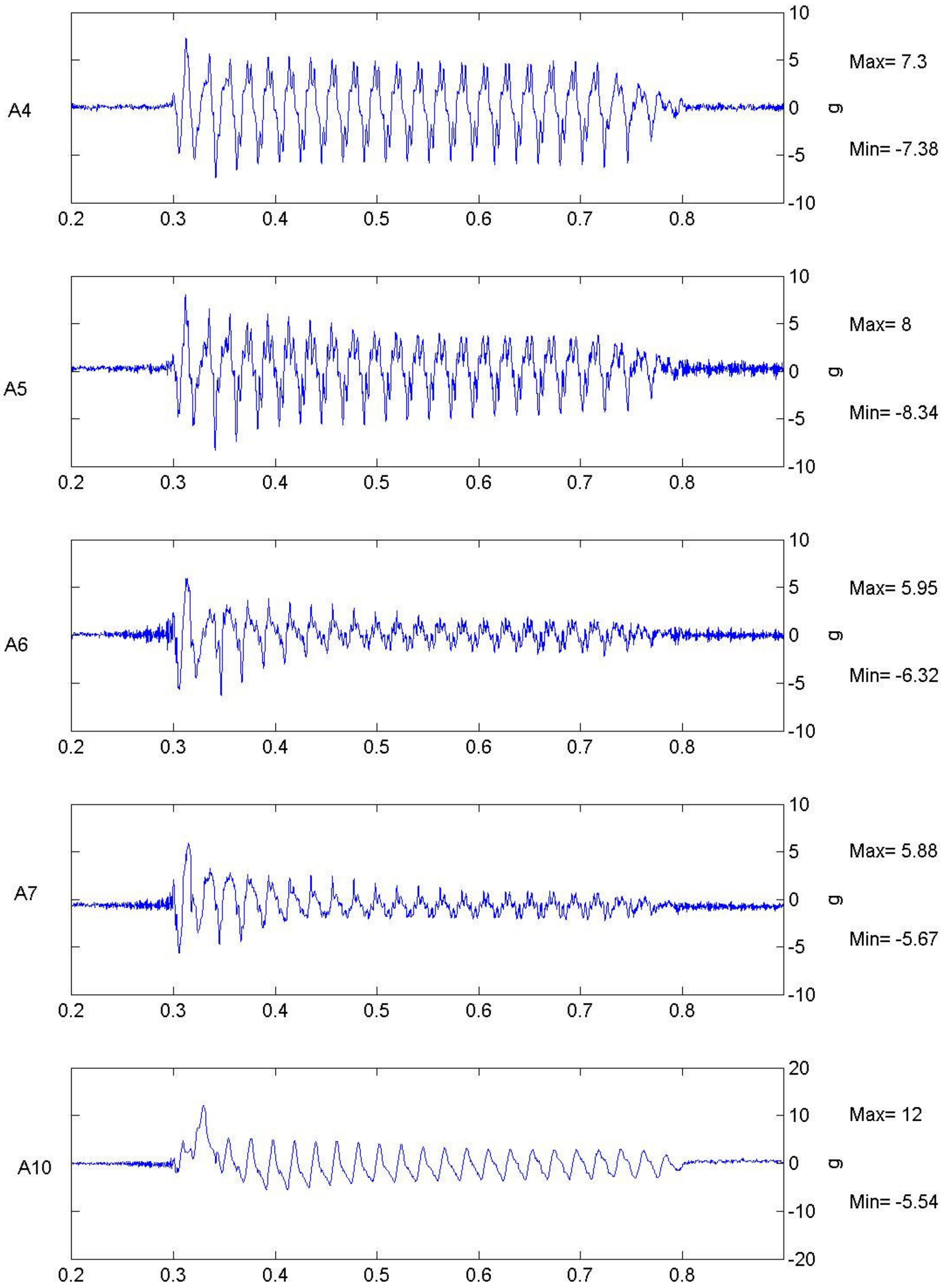

TEST BG-1 FLIGHT 1	**FREQ** **50 Hz**	Scales: Model 8th order Butterworth Filter at 1000Hz Short-Term Time Records	Earthquake 1	Figure No. 10

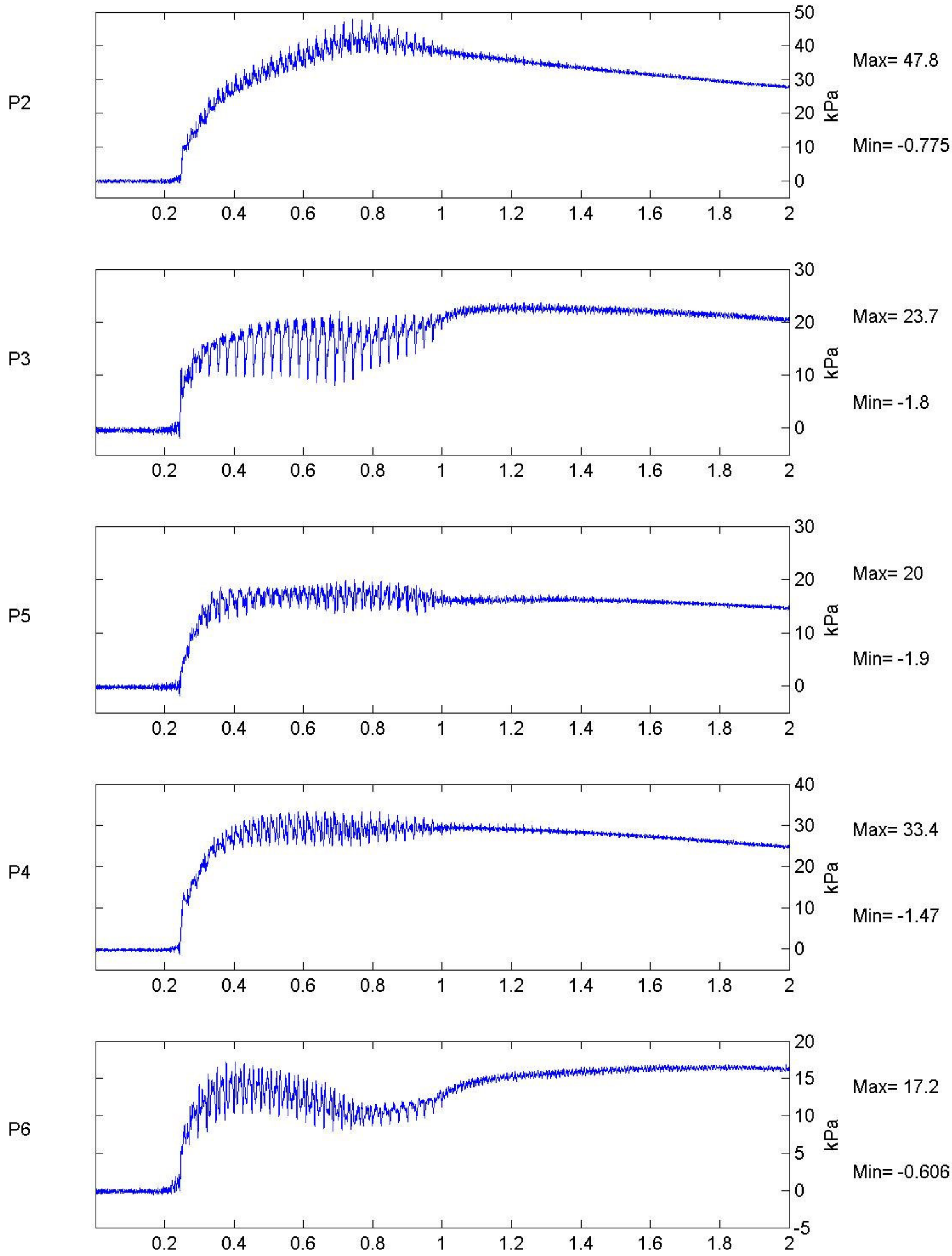

TEST BG-2 FLIGHT 1	**FREQ** **40 Hz**	Scales: Model Unfiltered Data Short-Term Time Records	Earthquake 2	Figure No. 11

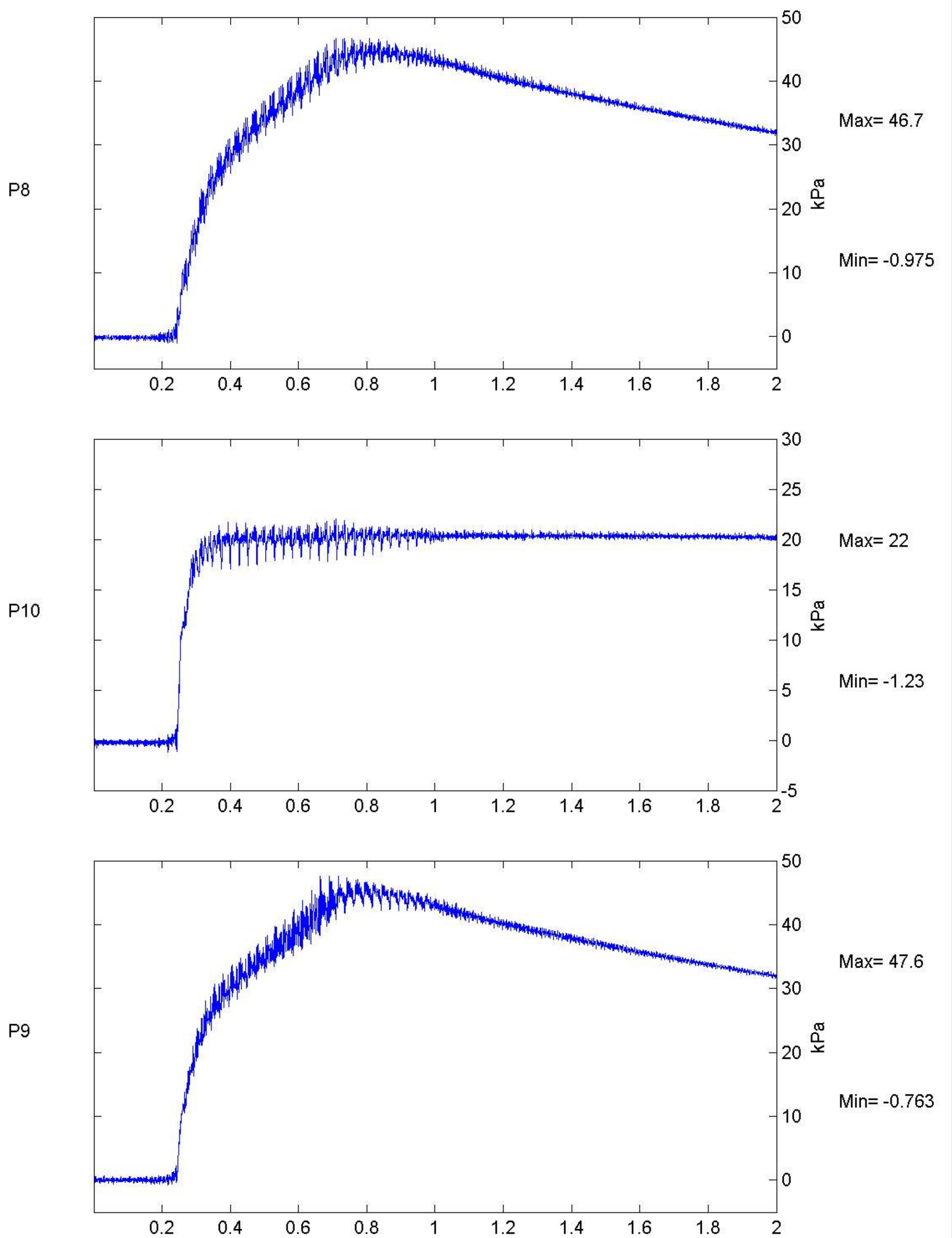

TEST BG-2 FLIGHT 1	**FREQ** **40 Hz**	Scales: Model Unfiltered Data Short-Term Time Records	Earthquake 2	Figure No. 12

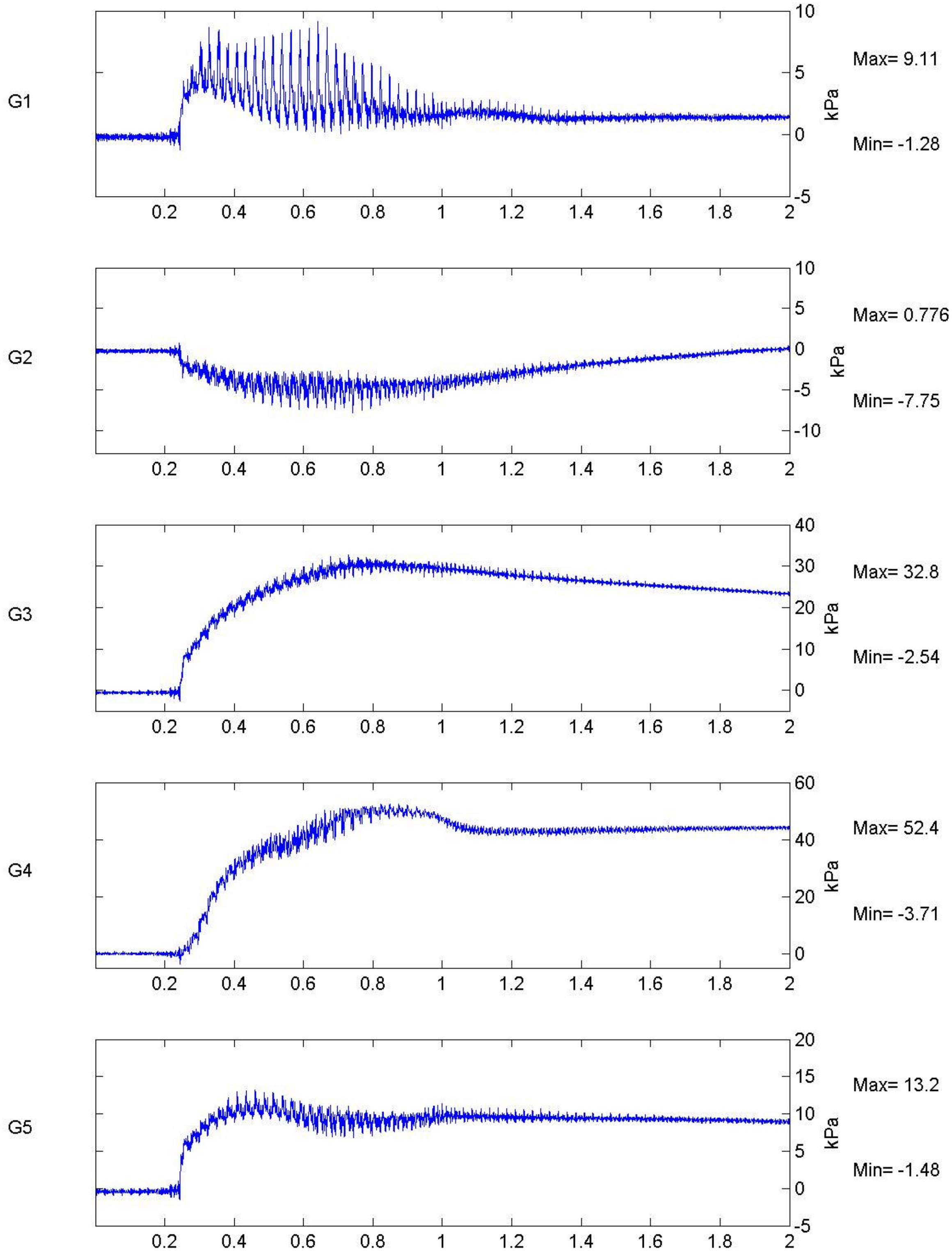

TEST BG-2	FREQ 40 Hz	Scales: Model Unfiltered Data	Earthquake	Figure No.
FLIGHT 1		Short-Term Time Records	2	13

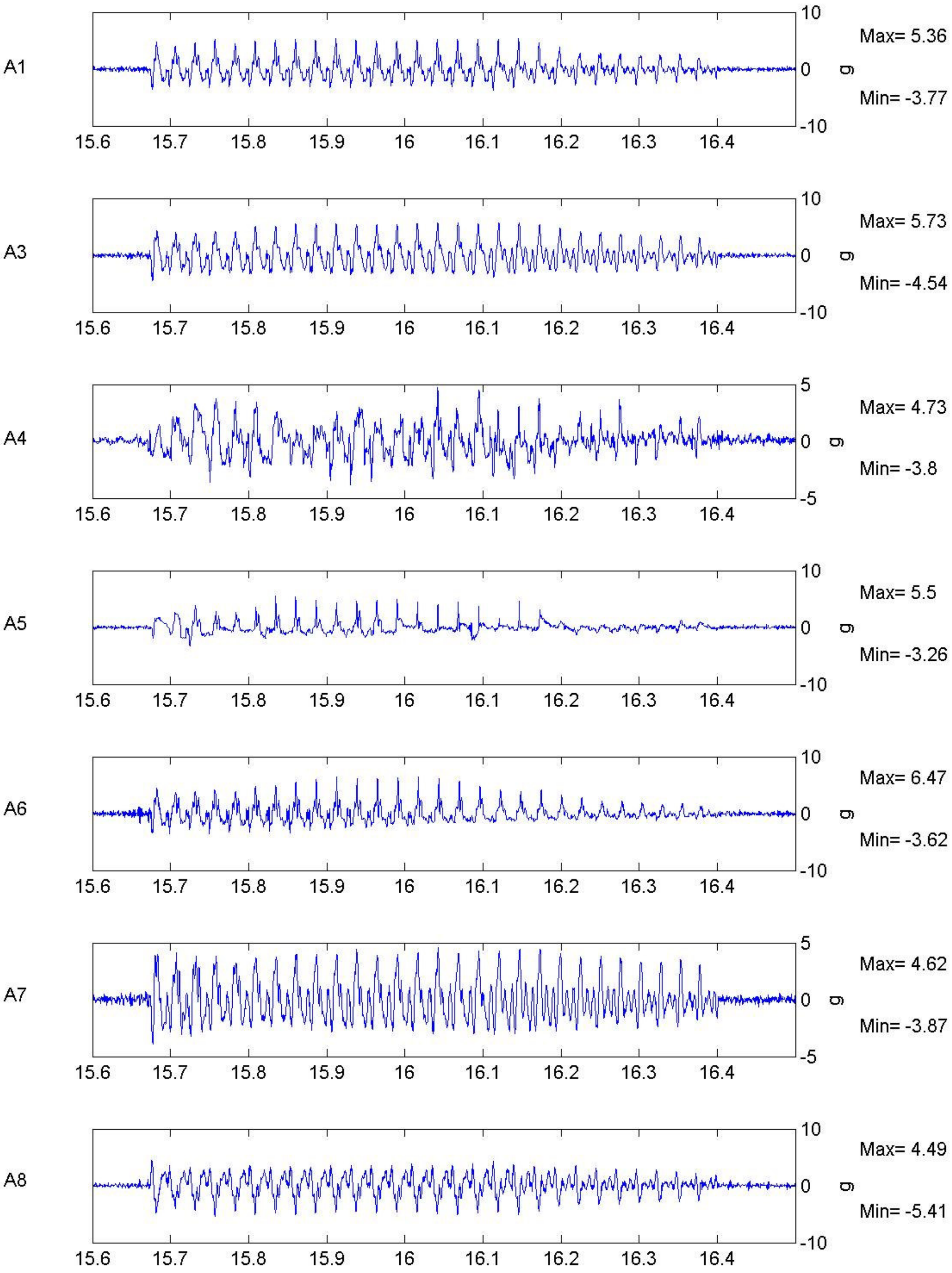

TEST BG-2 FLIGHT 1	**FREQ** **40 Hz**	Scales: Model 8th order Butterworth Filter at 1000Hz Short-Term Time Records	Earthquake 2	Figure No. 14

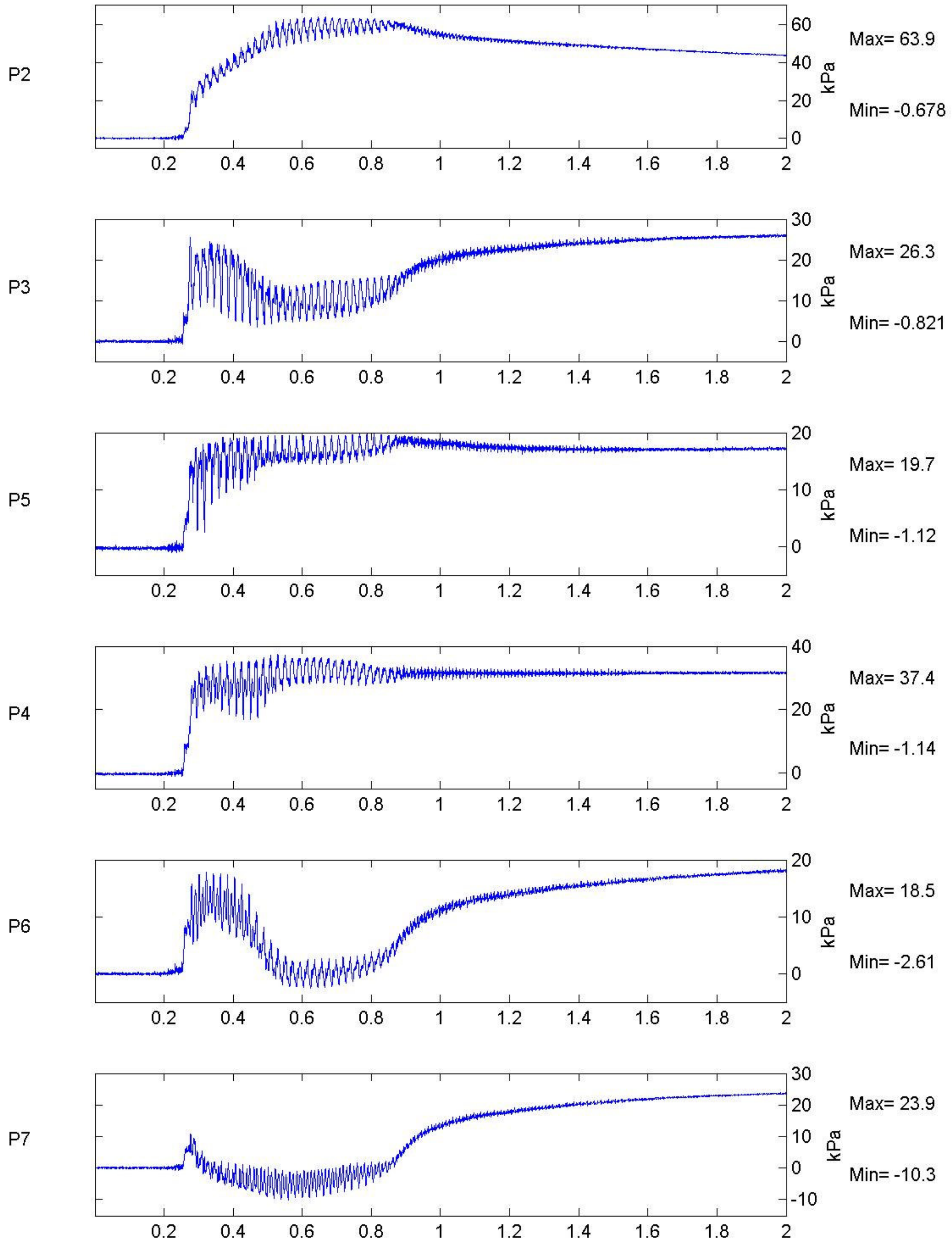

TEST BG-2	**FREQ 50 Hz**	Scales: Model Unfiltered Data	Earthquake	Figure No.
FLIGHT 1		Short-Term Time Records	3	15

P8

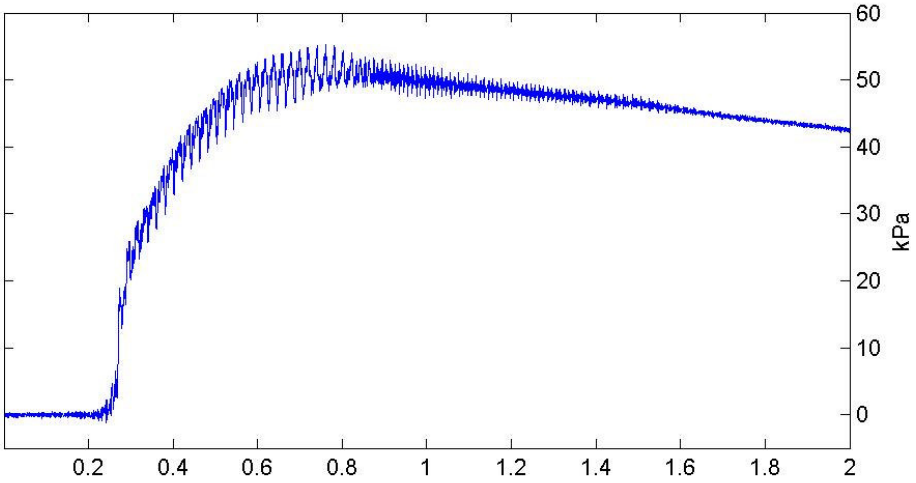

Max= 55.3

Min= -1.18

P10

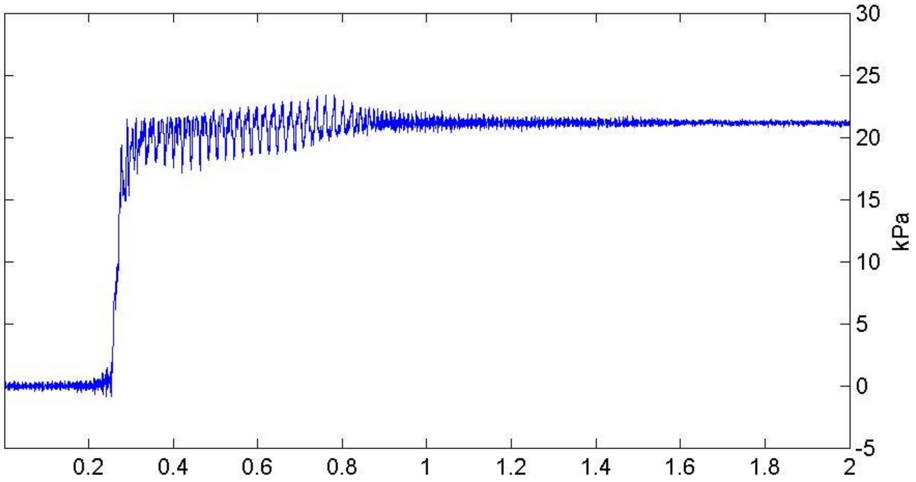

Max= 23.4

Min= -0.876

P9

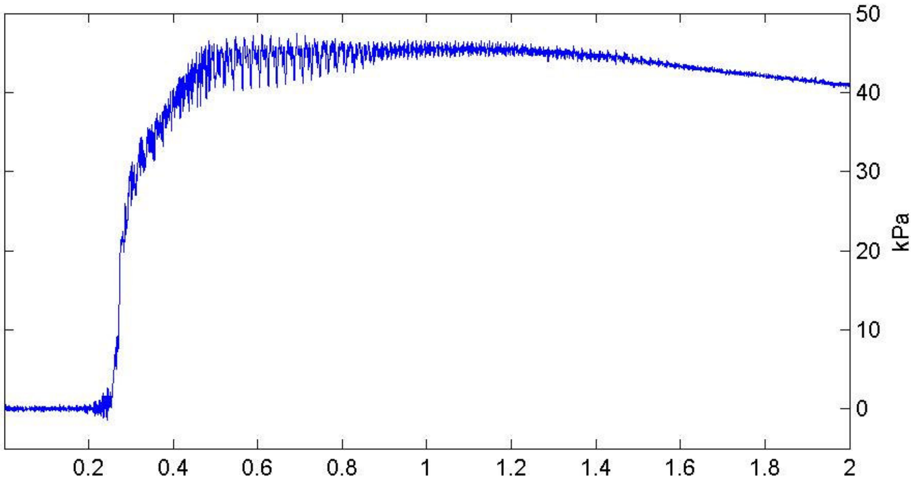

Max= 47.5

Min= -1.4

TEST BG-2 FLIGHT 1	**FREQ 50 Hz**	Scales: Model Unfiltered Data Short-Term Time Records	Earthquake 3	Figure No. 16

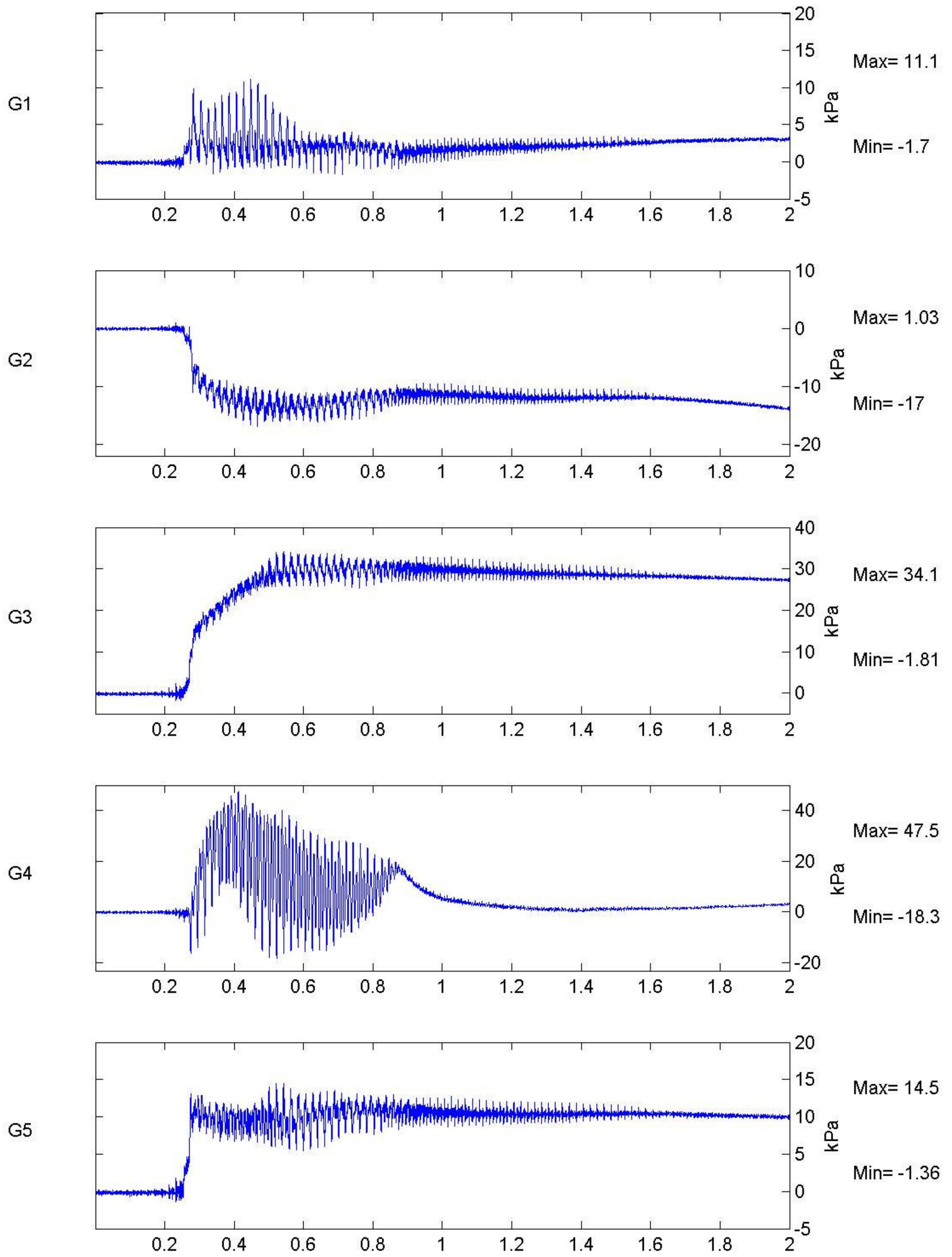

TEST BG-2 FLIGHT 1	**FREQ** **50 Hz**	Scales: Model Unfiltered Data Short-Term Time Records	Earthquake 3	Figure No. 17

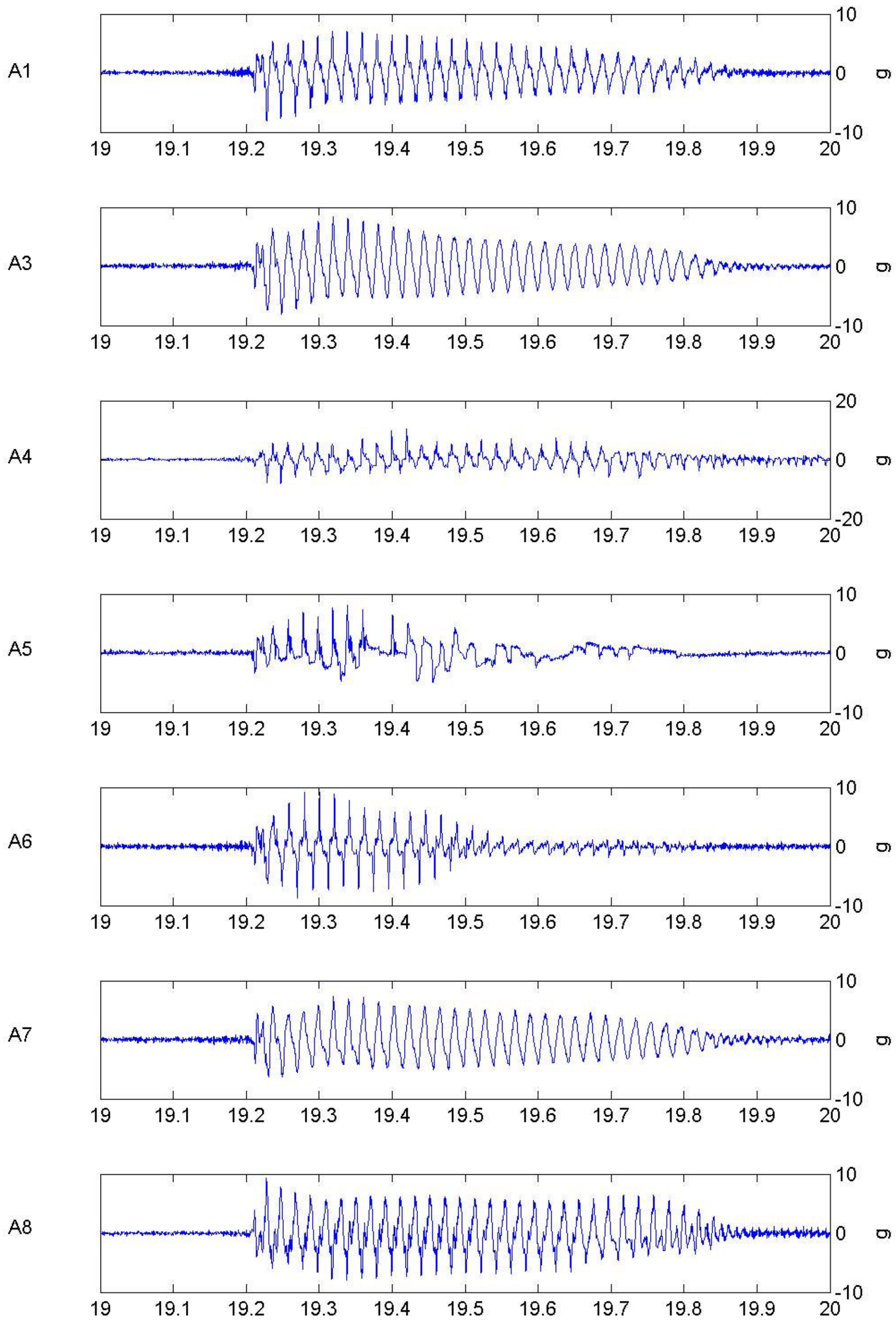

TEST BG-2 FLIGHT 1	**FREQ** **50 Hz**	Scales: Model 8th order Butterworth Filter at 1000Hz Short-Term Time Records	Earthquake 2	Figure No. 18

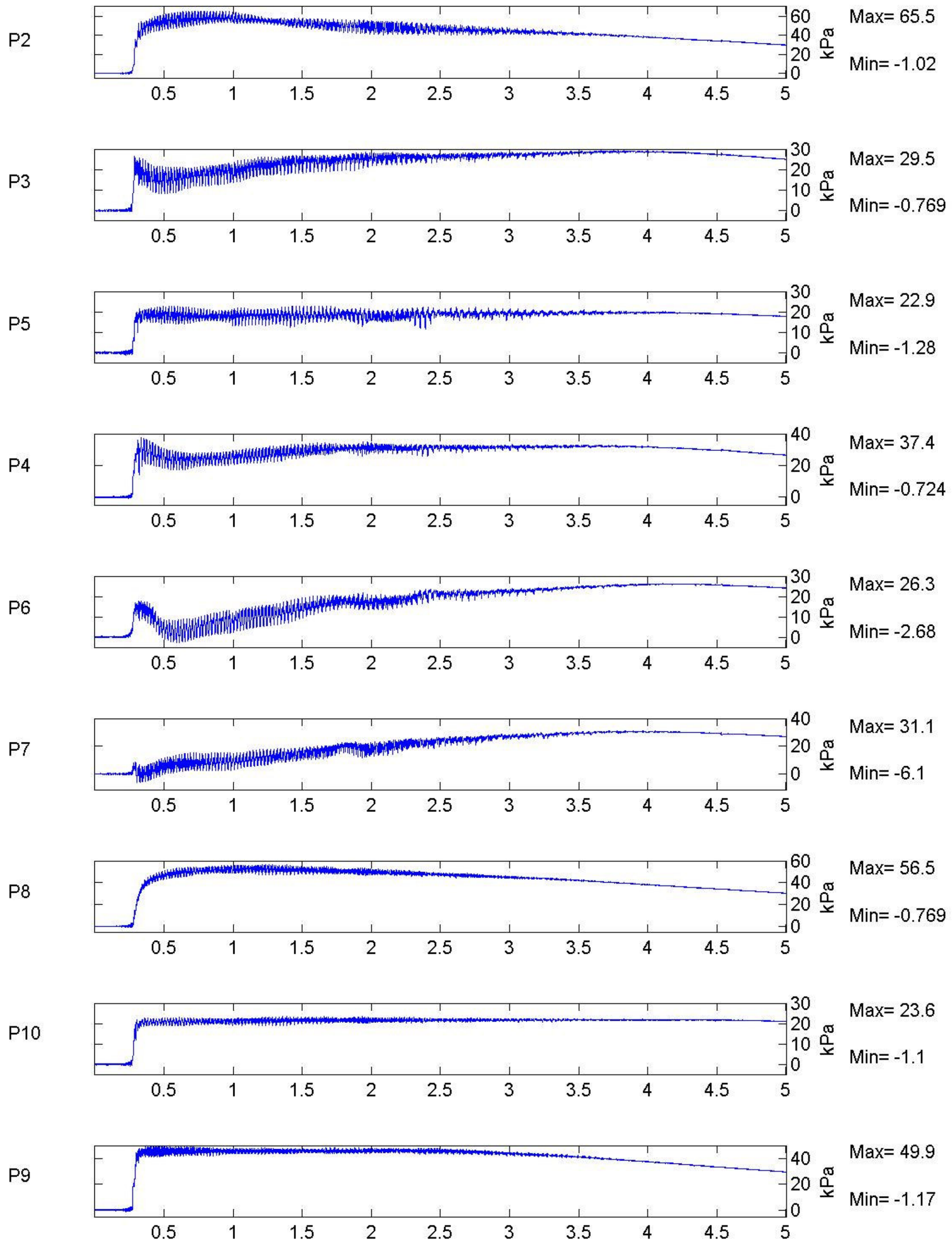

TEST BG-2 FLIGHT 1	SWEPT SINE WAVE	Scales: Model Unfiltered Data Long-Term Time Records	Earthquake 4	Figure No. 19

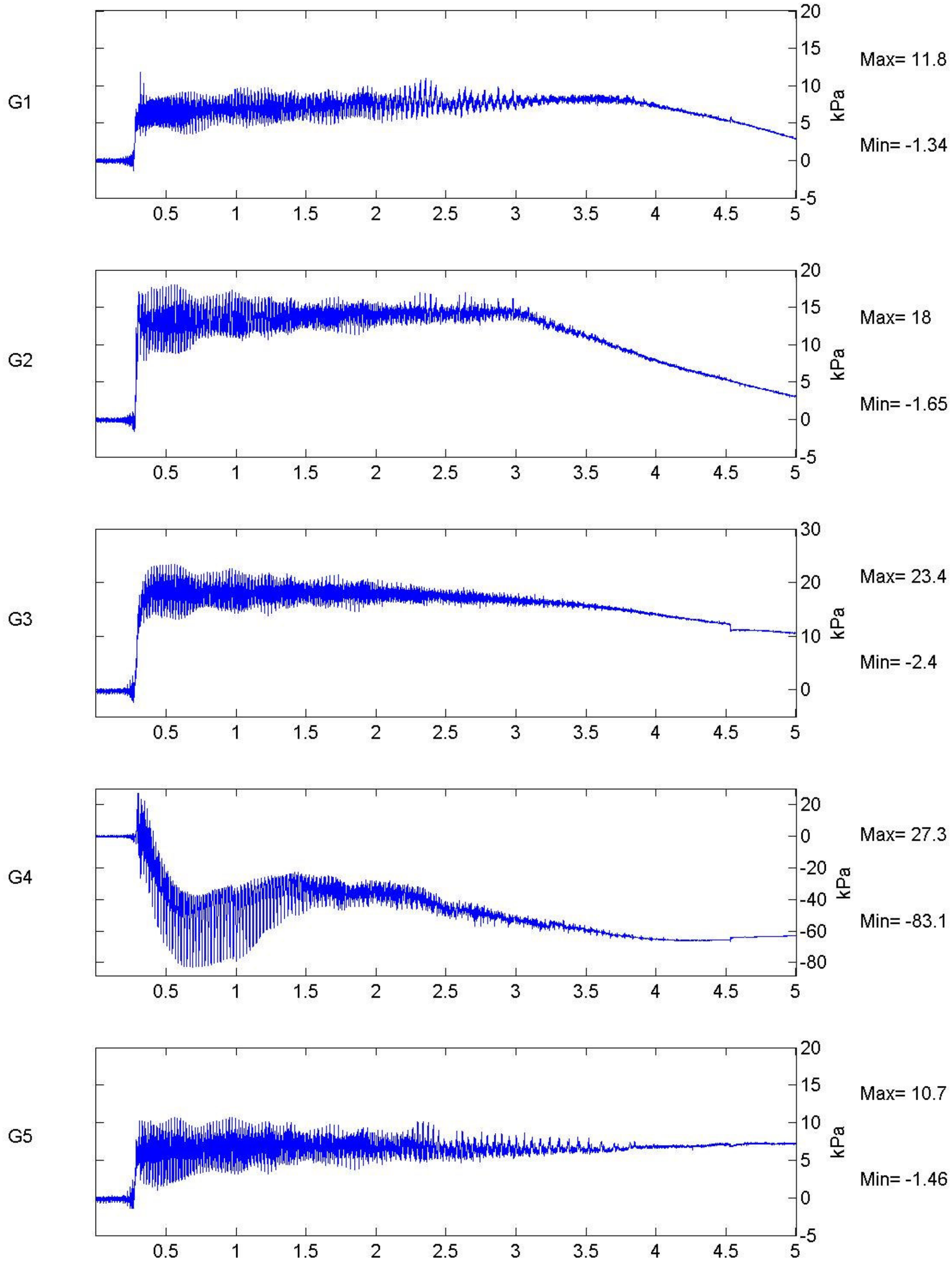

TEST BG-2 FLIGHT 1	**SWEPT SINE WAVE**	Scales: Model Unfiltered Data Long-Term Time Records	Earthquake 4	Figure No. 20

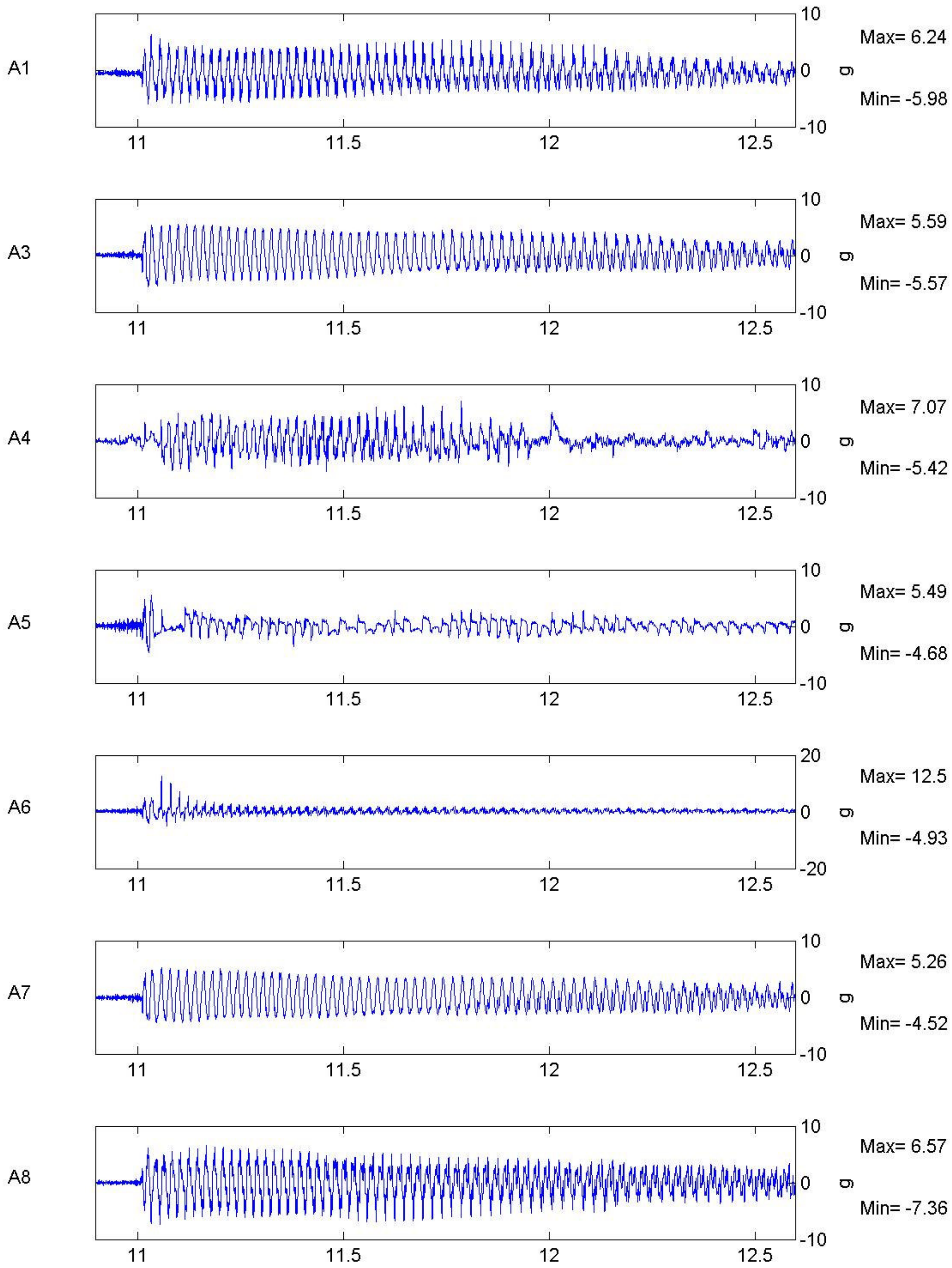

TEST BG-2 FLIGHT 1	**SWEPT SINE WAVE**	Scales: Model 8th order Butterworth Filter at 1000Hz Short-Term Time Records	Earthquake 3	Figure No. 21

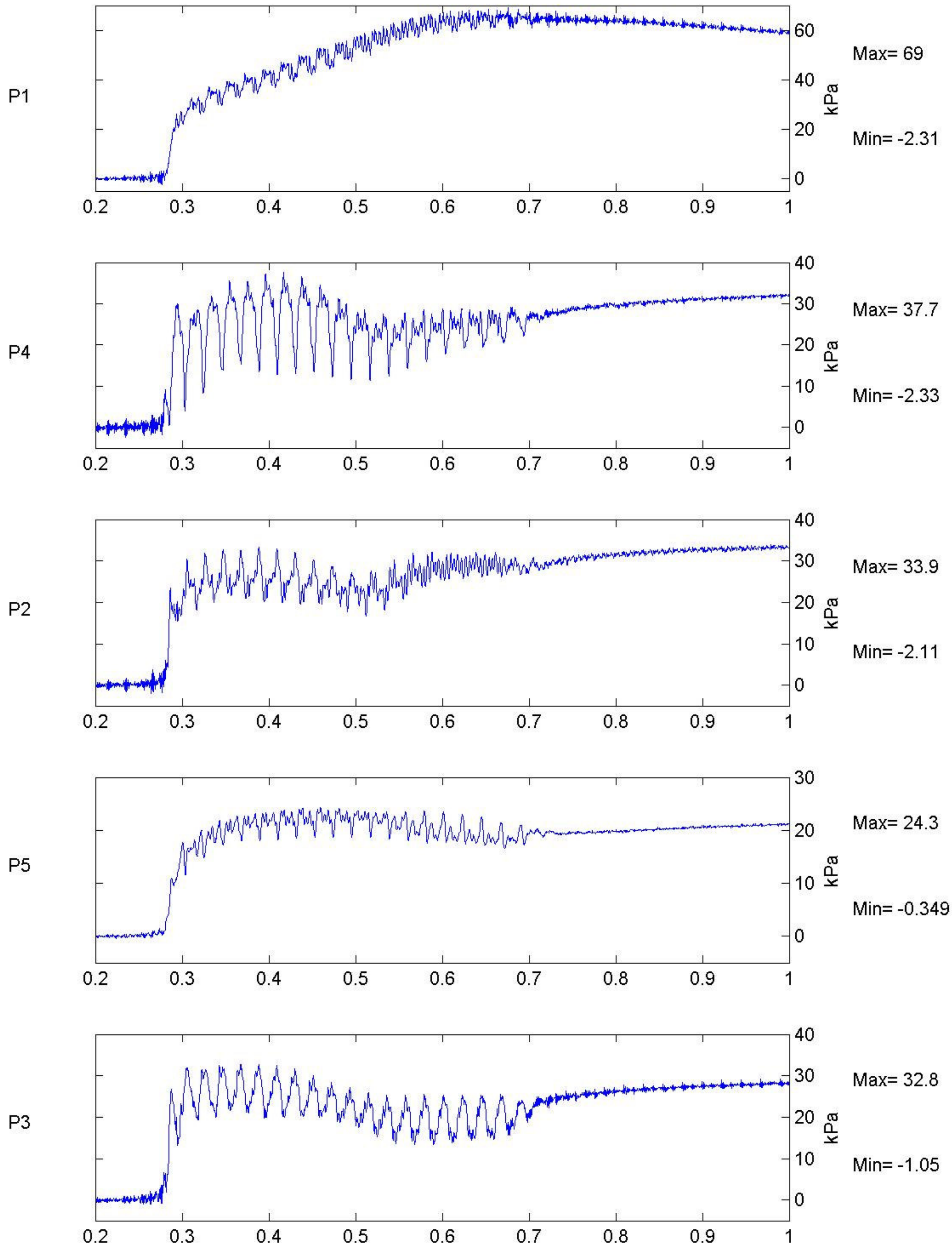

TEST BG-03 FLIGHT 1	**FREQ** **50 Hz**	Scales: Model Unfiltered Data Short-Term Time Records	Earthquake 3	Figure No. 22

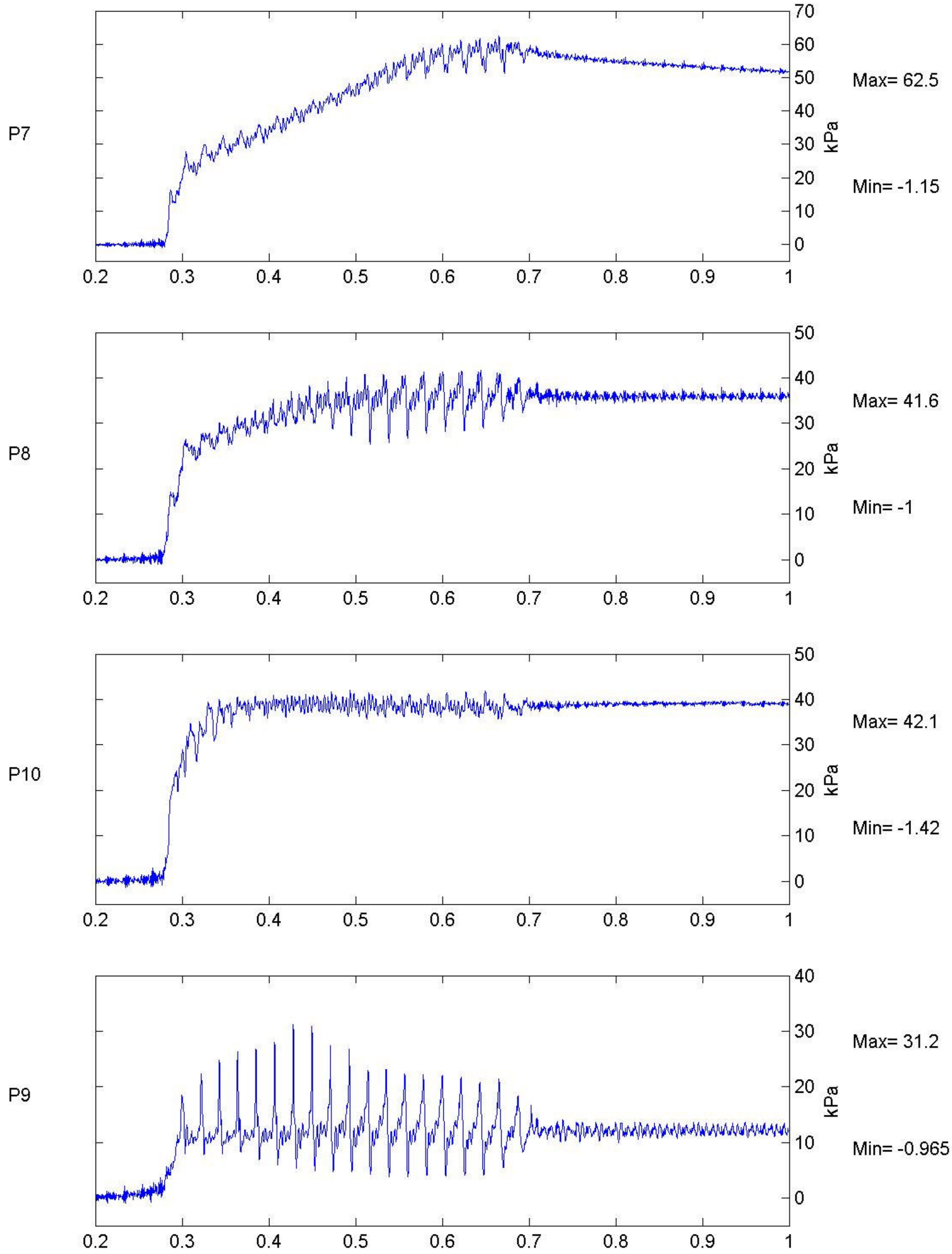

TEST BG-03 FLIGHT 1	**FREQ** **50 Hz**	Scales: Model Unfiltered Data Short-Term Time Records	Earthquake 3	Figure No. 23

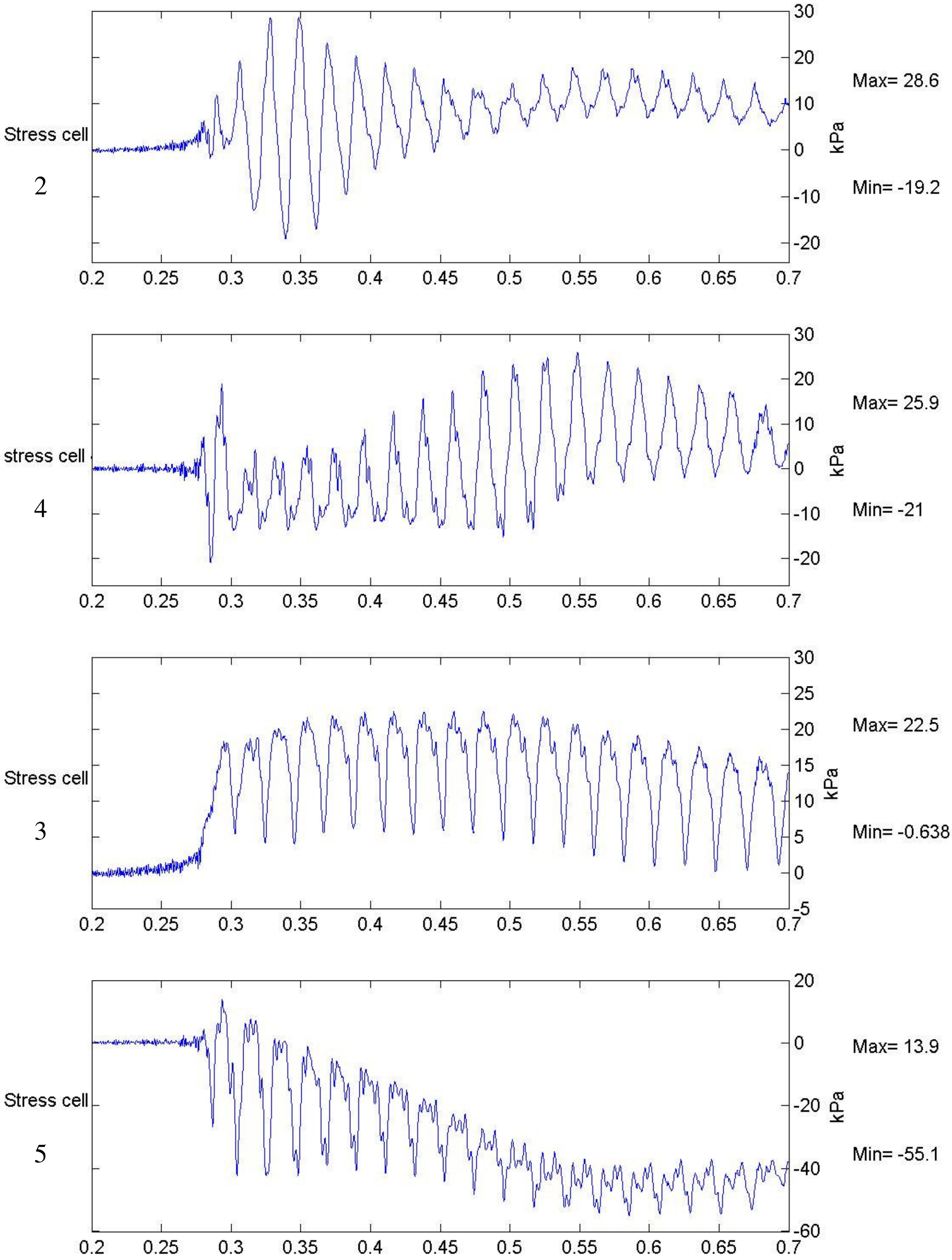

TEST BG-03 FLIGHT 1	**FREQ 50 Hz**	Scales: Model Unfiltered Data Short-Term Time Records	Earthquake 3	Figure No. 24

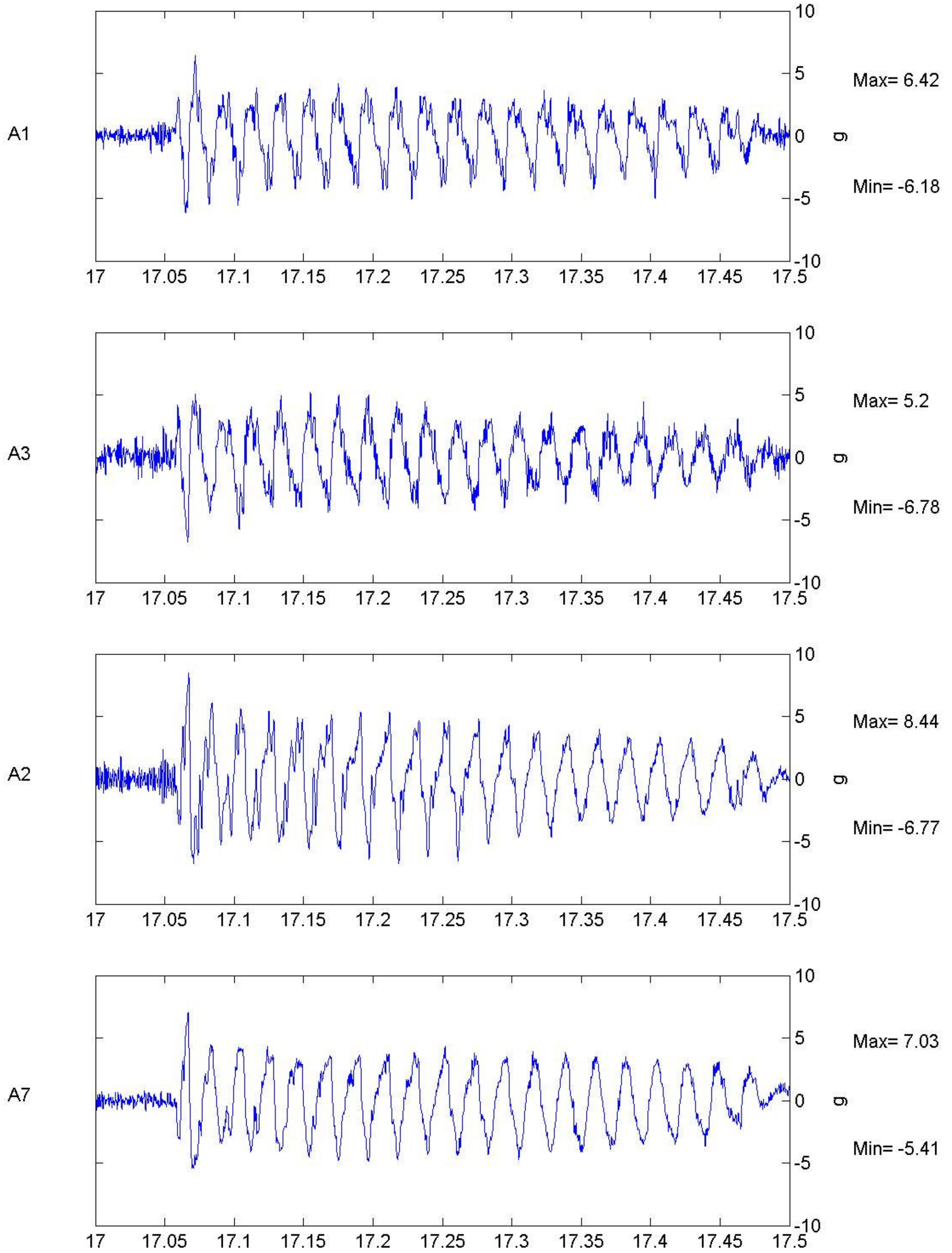

TEST BG-03 FLIGHT 1	**FREQ 50 Hz**	Scales: Model 8th order Butterworth Filter at 1000Hz Short-Term Time Records	Earthquake 3	Figure No. 25

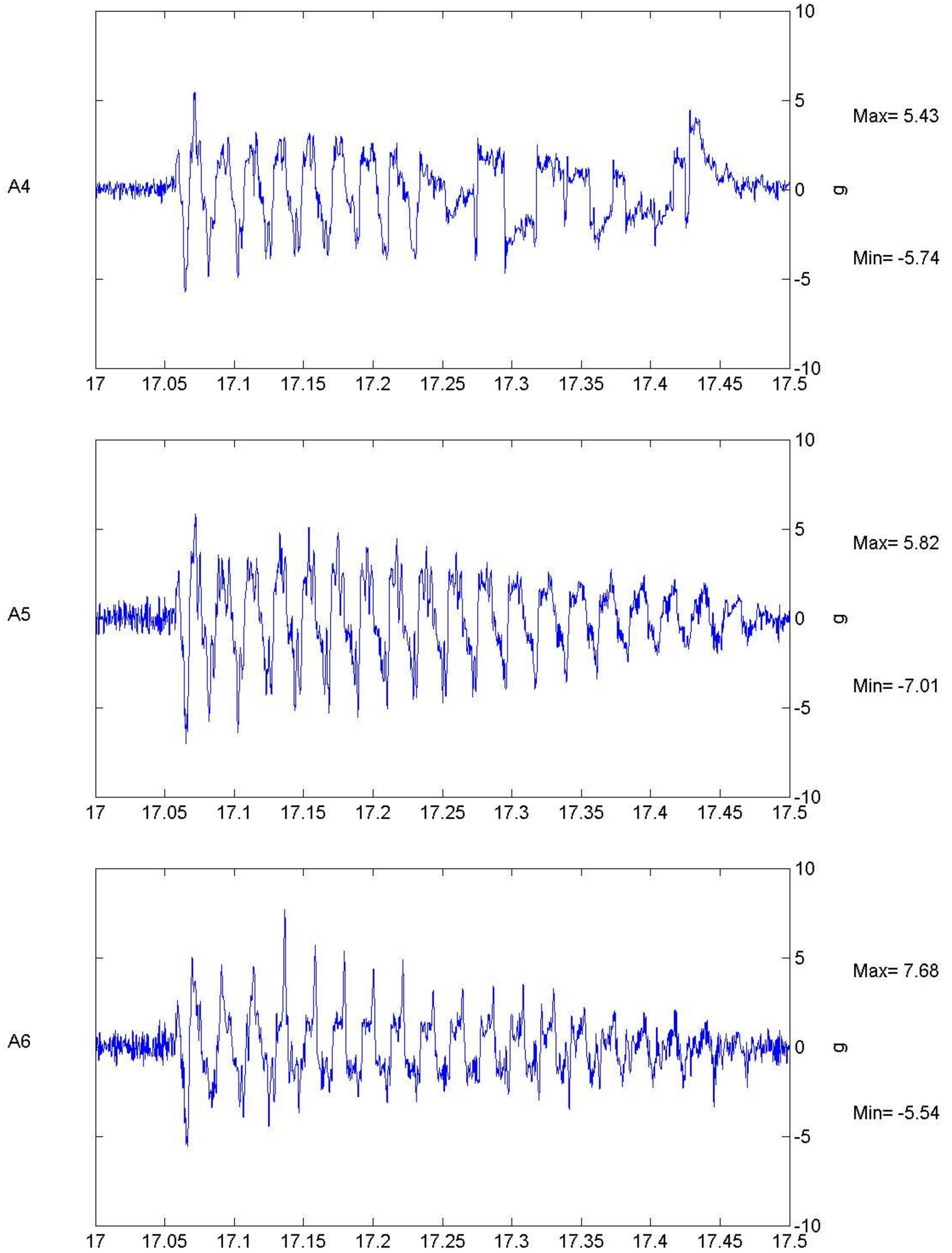

TEST BG-03 FLIGHT 1	**FREQ** **50 Hz**	Scales: Model 8th order Butterworth Filter at 1000Hz Short-Term Time Records	Earthquake 3	Figure No. 26

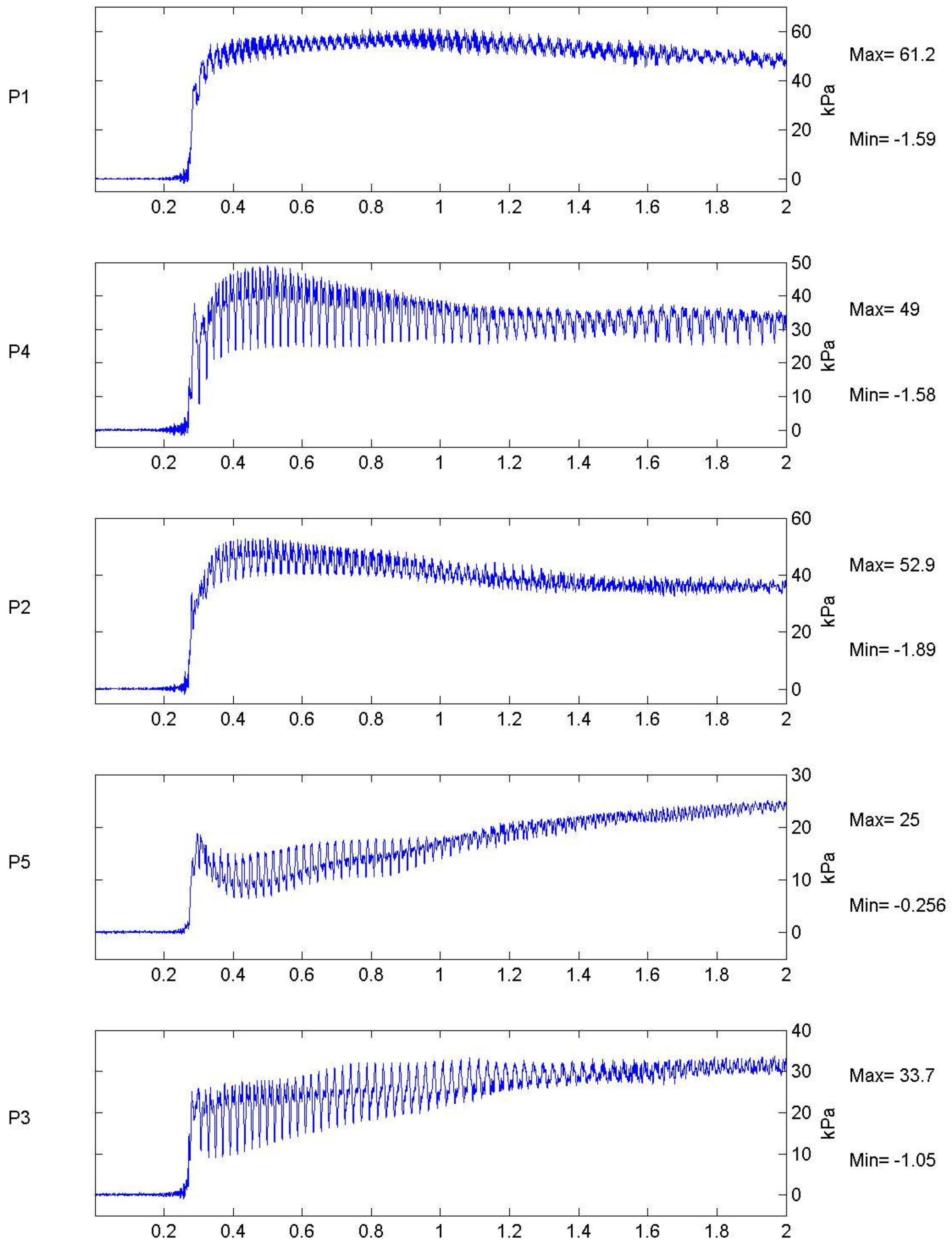

TEST BG-03 FLIGHT 1	SWEPT SINE WAVE	Scales: Model Unfiltered Data Short-Term Time Records	Earthquake 4	Figure No. 27

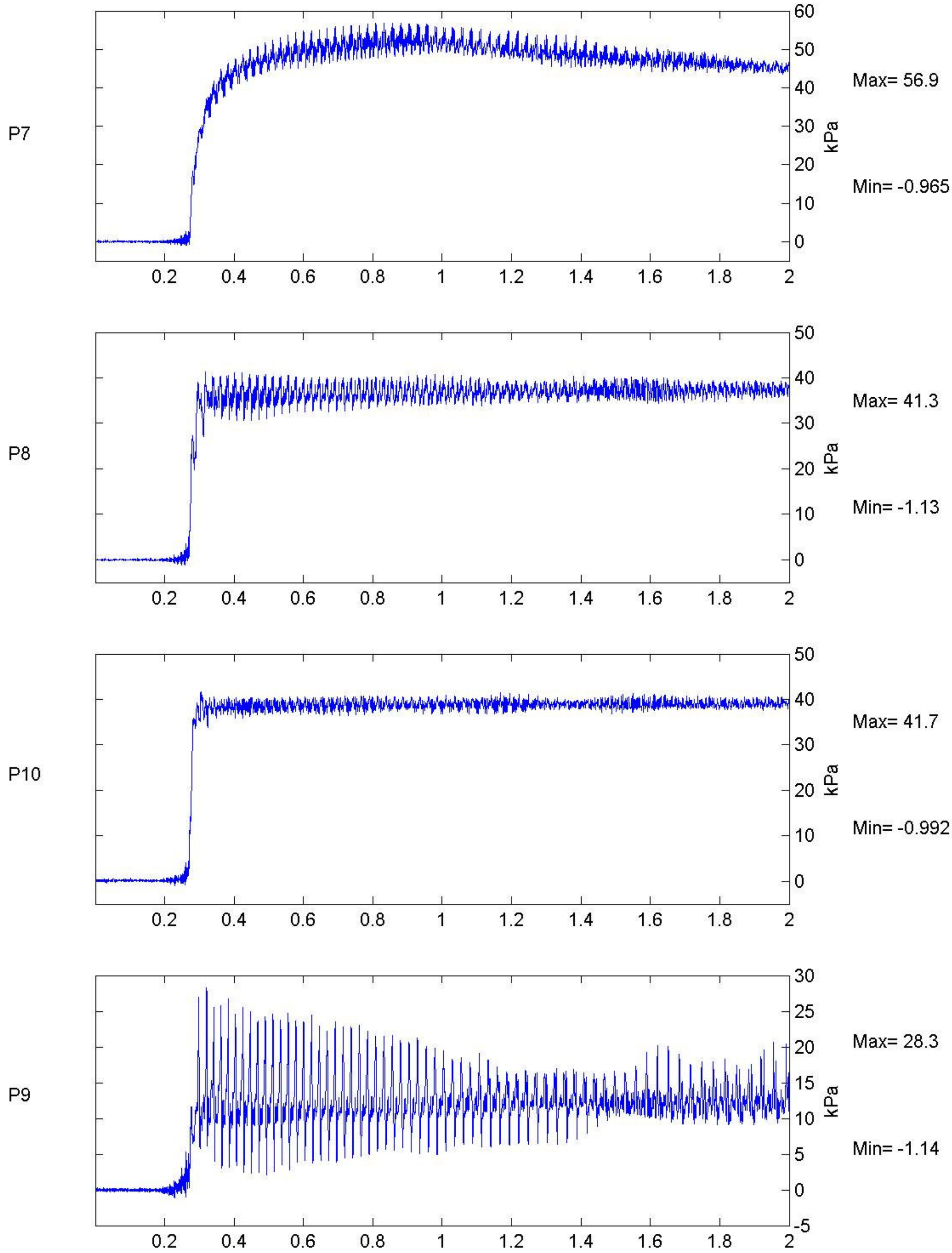

TEST BG-03 FLIGHT 1	**SWEPT SINE WAVE**	Scales: Model Unfiltered Data Short-Term Time Records	Earthquake 4	Figure No. 28

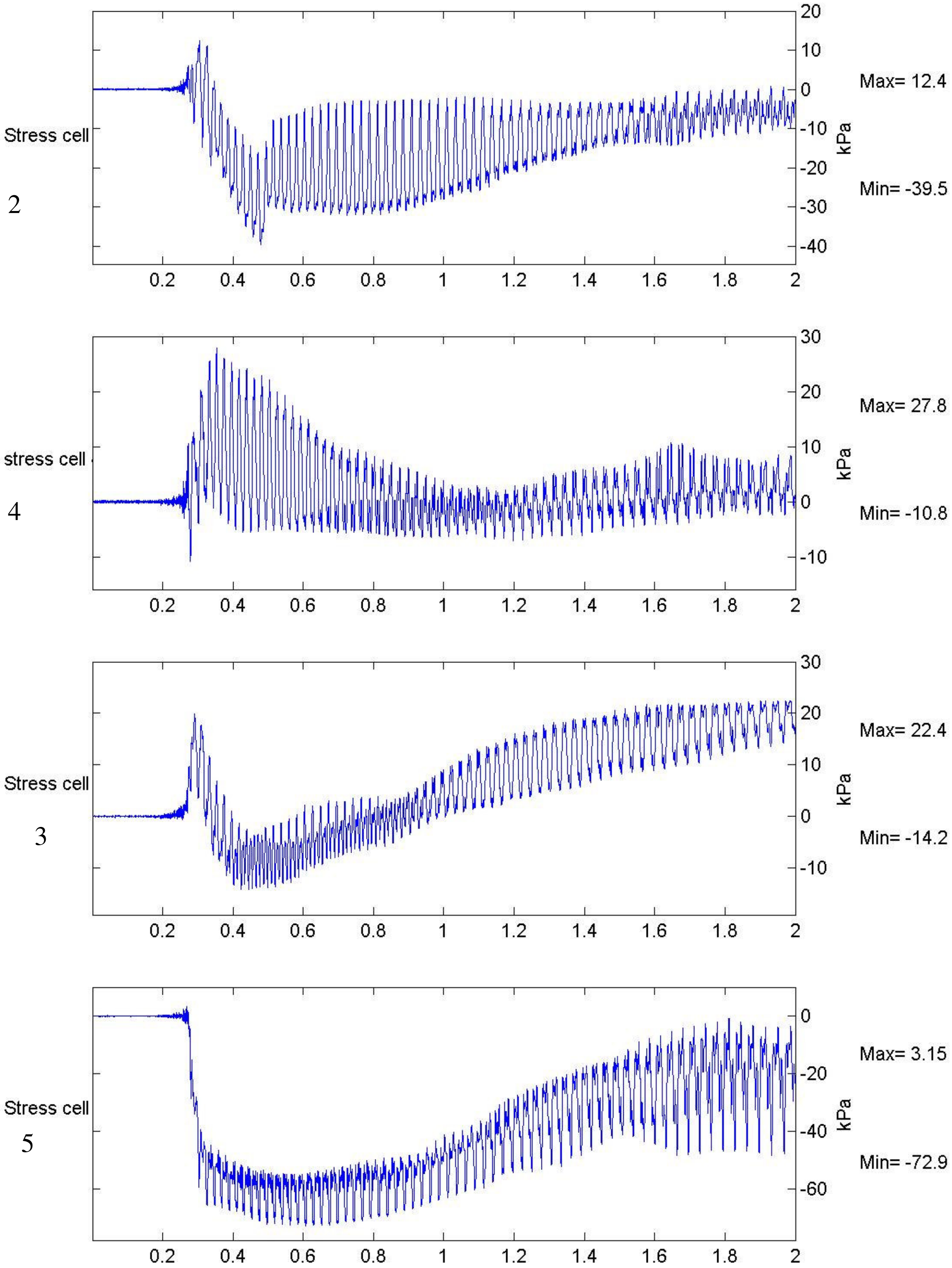

TEST BG-03 FLIGHT 1	SWEPT SINE WAVE	Scales: Model Unfiltered Data Short-Term Time Records	Earthquake 4	Figure No. 29

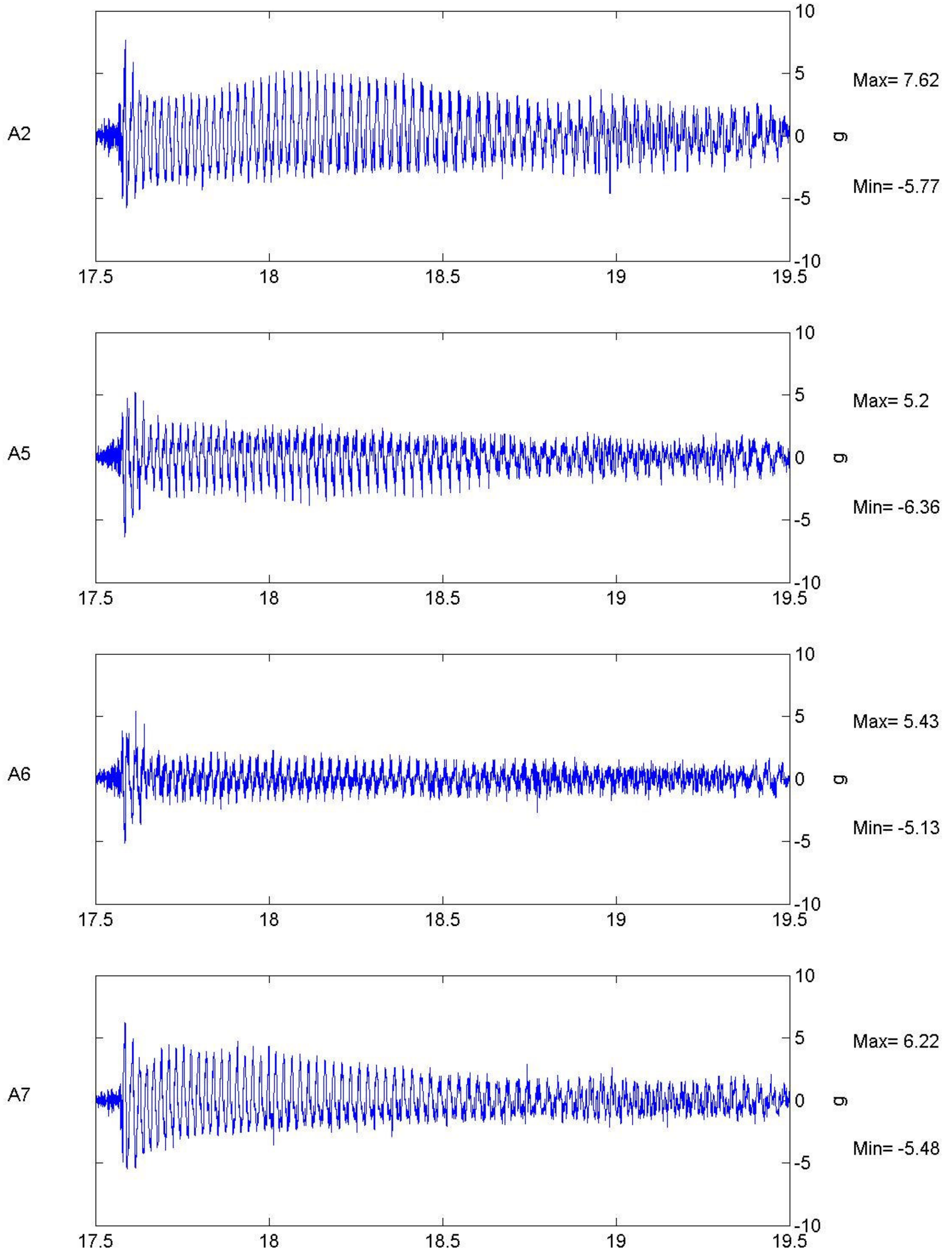

TEST BG-03 FLIGHT 1	SWEPT SINE WAVE	Scales: Model 8th order Butterworth Filter at 1000Hz Long-Term Time Records	Earthquake 4	Figure No. 30

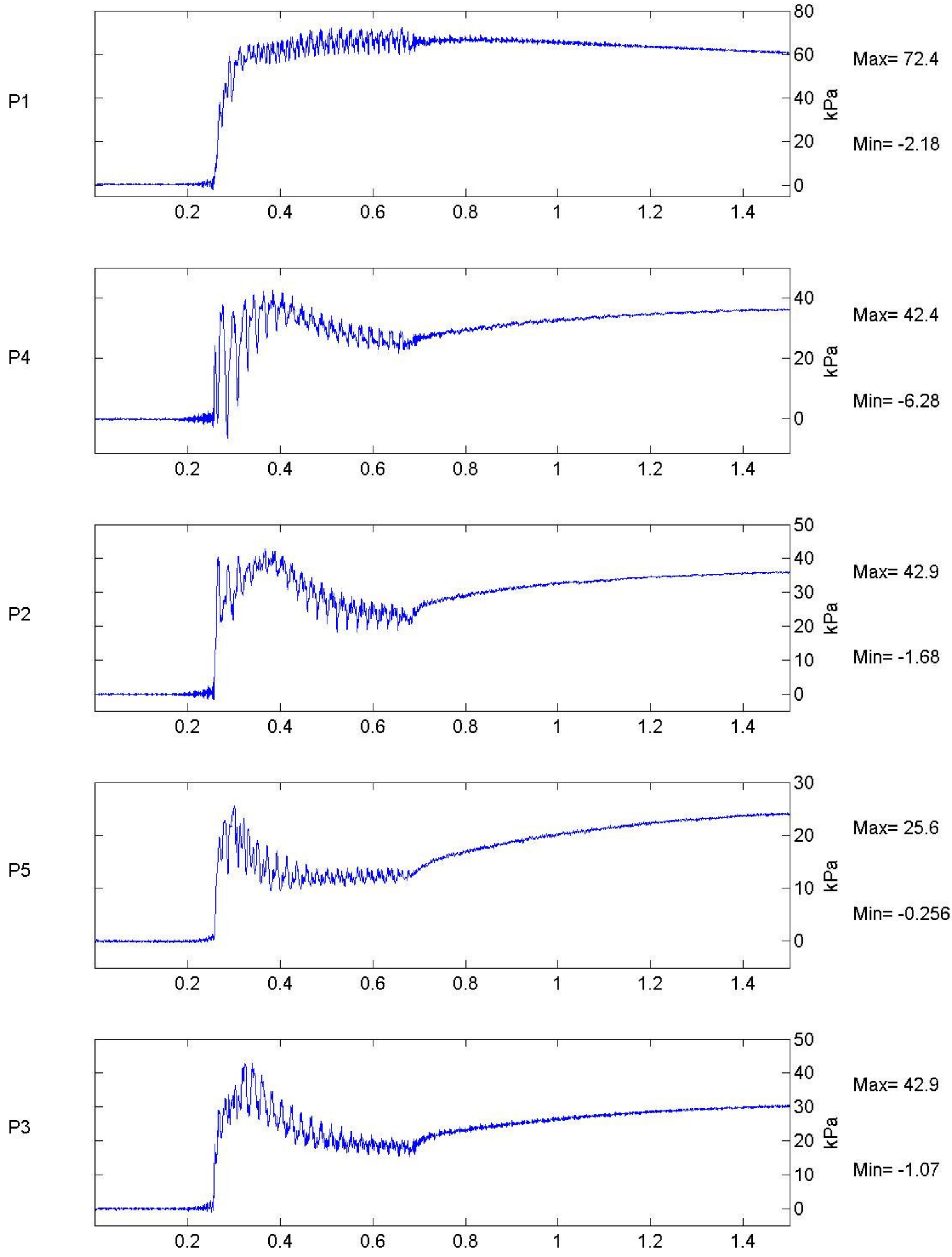

TEST BG-03 FLIGHT 1	**FREQ** **50 Hz**	Scales: Model Unfiltered Data Short-Term Time Records	Earthquake 5	Figure No. 31

P7

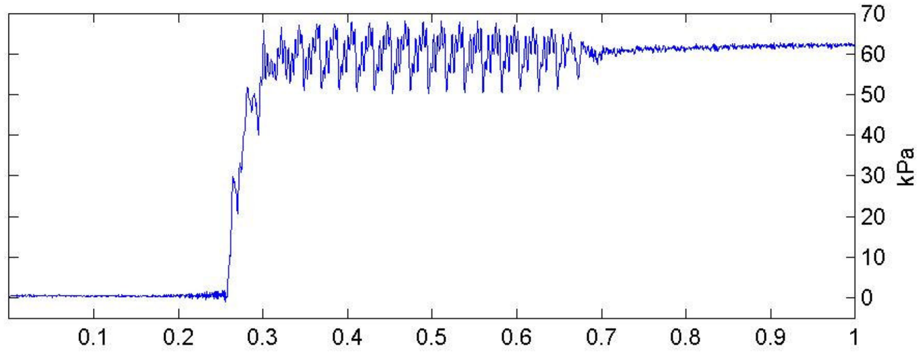

P8

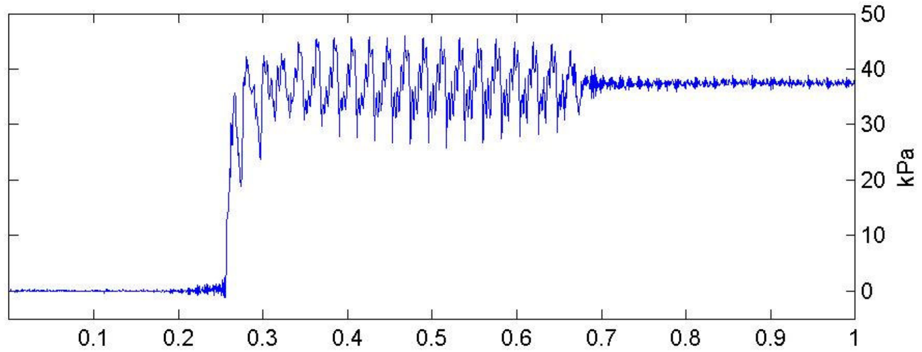

P10

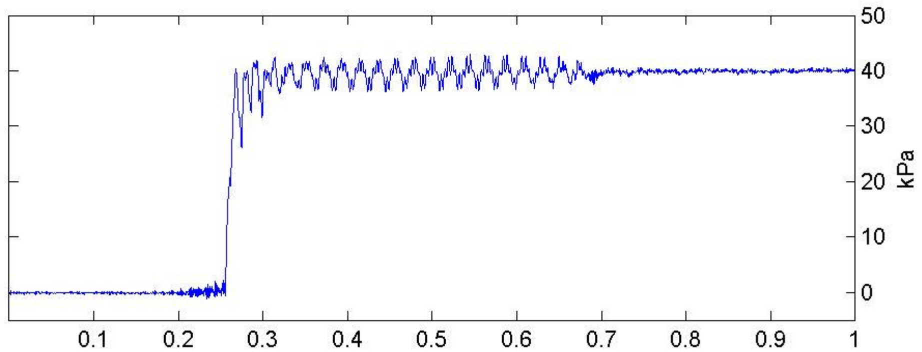

P9

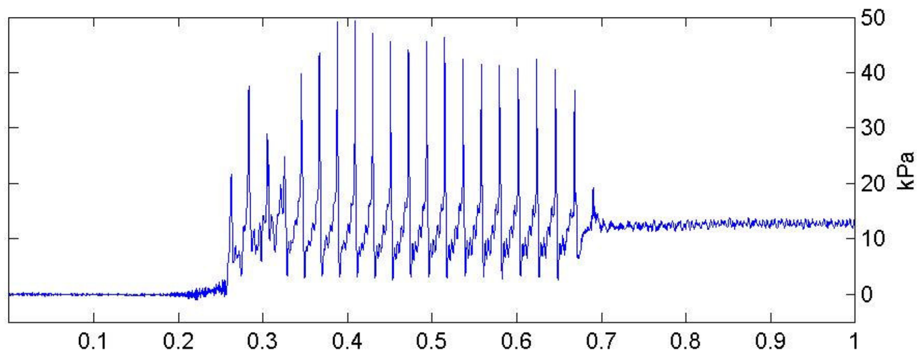

TEST BG-03 FLIGHT 1	**FREQ** **50 Hz**	Scales: Model Unfiltered Data Short-Term Time Records	Earthquake 5	Figure No. 32

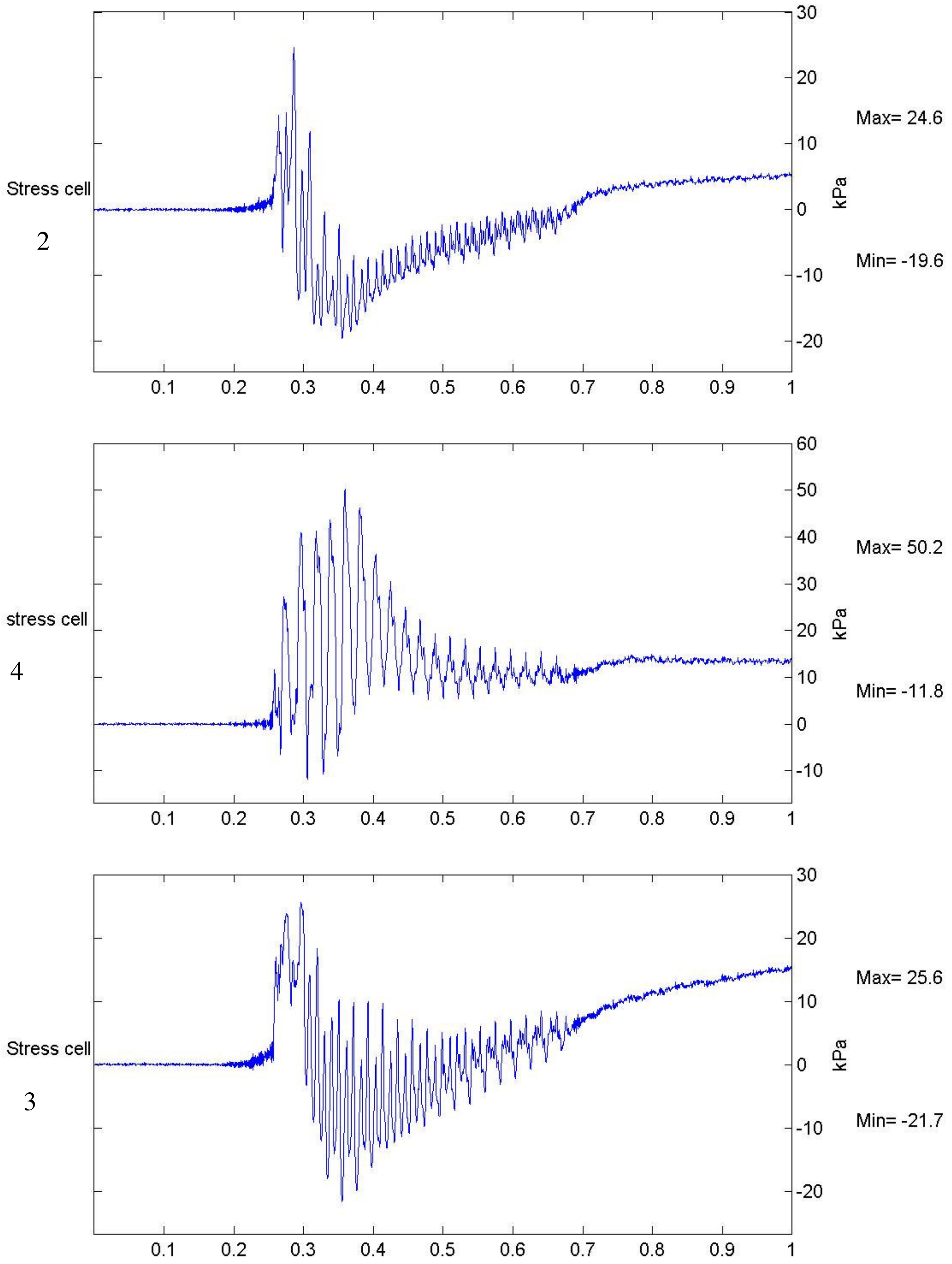

TEST BG-03 FLIGHT 1	**FREQ** **50 Hz**	Scales: Model Unfiltered Data Short-Term Time Records	Earthquake 5	Figure No. 33